Characterization of Dominant Negative Asp11 Mutant Actins

July 2014

Jun NAKAJIMA

Characterization of Dominant Negative Asp11 Mutant Actins

A Dissertation Submitted to
the Graduate School of Life and Environmental Sciences,
the University of Tsukuba
in Partial Fulfillment of the Requirements
for the Degree of Doctor of Philosophy in Science
(Doctoral Program in Structural Biosciences)

Jun NAKAJIMA

Table of contents

List of figures

Abstract

Polymerization and depolymerization of actin filaments in cells are controlled in time and space, and proteins of the ADF / cofilin family are generally considered to play important roles in these processes. However, there are still many questions about the regulatory mechanism of interactions between ADF/cofilin proteins and actin filaments. For example, the depolymerizing activities by ADF/cofilin proteins from plants and *Acanthamoeba* are reported to depend on nucleotide that is bound to actin subunits in filaments, but the physiological significance and generality of such a control mechanism is unclear. Asp11 is conserved in all actins, and interacts with ß- and γ-phosphate groups of ATP through a divalent cation. Among the mutants of this Asp11, D11Q mutation is dominant lethal in yeast actin, and D11N mutation in α-actin dominantly causes congenital myopathy in human. It is expected that functional analysis of dominantly toxic mutant actins such as these would provide useful information to elucidate the mechanism of interaction between cofilin and actin with a focus on the nucleotide state. However, it is difficult to obtain large quantities of dominantly toxic mutant actins, and therefore, detailed functional analysis of the Asp11 mutant actins have not been performed yet. This situation recently changed, since it became possible to purify relatively large amounts of dominantly toxic mutant actin by using a unique expression system developed in the laboratory that I belong to. In this study, I first examined the affinity between actin filaments and human cofilin under different conditions of the actin-bound nucleotides. Then, together with my colleagues of the laboratory, I performed detailed functional analysis of the D11N and D11Q mutant actins. Based on the results, I conjectured why those Asp11 mutant actins show dominant toxicity, in a manner related to the actin-bound nucleotide state.

Below is a brief outline of this thesis.

In General Introduction, I summarized what is known about actin, regulation of polymerization and depolymerization of actin, and cofilin's roles in those processes.

In Chapter I entitled "Effects of bound nucleotide on the affinity of actin for cofilin", I report how the affinity between actin filaments and cofilin

changes when the actin-bound nucleotide state was changed experimentally. The experiments were carried out using a fluorescence microscope and actin and cofilin each labeled with two different fluorophores, respectively. Importantly, unlike the case with ADP-bound actin filaments, filaments carrying ADP and Pi hardly bound cofilin. Furthermore, I was able to observe cooperative binding of cofilin to actin filaments carrying ADP. Cooperative binding of cofilin to actin filaments has been observed by electron microscopy, and the present results not only confirmed those electron microscopic studies with fluorescence microscopy, but also showed that the cooperative binding occurs in the micrometer range of lengths.

In Chapter Ⅱ entitled "Characterization of Dominant Negative Asp11 Mutant Actins", I conducted functional analyses of D11N and D11Q mutant actins. These mutant actins exhibited polymerization competence that was similar to that of the wild-type, but depolymerization of the mutant filaments, as well as copolymer of the mutant and wild type actins, were slower than the wild type filaments, regardless of whether the depolymerization was spontaneous or induced by cofilin. In addition, the rates of Pi release and nucleotide exchange of D11N and D11Q actins were measured by my colleagues of the laboratory. Interestingly, while the ability to hydrolyze the bound ATP was normal, the exchange rate of bound nucleotide was much faster with the mutants than the wild type. From these results, I speculated that Asp11 mutant actins, such as D11N and D11Q, become dominantly toxic because the exchange of bound nucleotide with ATP present in the external solution is very quick, so that the majority of the mutant actin subunits in filaments carry ATP and therefore does not bind cofilin. This would result in a large amount of hard-to-depolymerize actin filaments, which would be highly toxic for the cells. In other words, this study demonstrated the significance of very slow nucleotide exchange when actin molecules are incorporated into filaments.

Finally, General Discussion summarizes the results of Chapter Ⅰ and Ⅱ. In addition, I discussed possible implication of my findings in a more general context of the regulation of actin cytoskeleton.

General Introduction

ACTIN

Actin was discovered in 1942 from rabbit skeletal muscle as activator protein for myosin (Straub, 1942). Subsequently, it was shown that actin is not specific to skeletal muscle, but is universally present in eukaryotic cells (e.g., Hatano and Oosawa, 1966). It is now known that actin plays essential roles in a number of important cellular processes, including cell migration (reviewed by Mitchison and Cramer, (1996)), cytokinesis (reviewed by Glotzer, (2001)), organelle transport (reviewed by Goode et al., (2000)) and transcriptional regulation in nucleus (Hendzel, 2014), through interaction with various actin-binding proteins. Furthermore, it is now well established that actin homologues are widely distributed in bacteria and archea (van den Ent et al., 2001).

Rabbit skeletal muscle actin consists of 375 amino acid residues, and its amino acid sequence is highly conserved throughout eukaryotic actins. For example, sequences of rabbit skeletal actin and yeast actin are 87% identical. In terms of structure (Kabsch et al., 1990), an actin molecule consists of large and small domains, each of which is divided into two subdomains, forming a large cleft between them (Fig. 1). A nucleotide-binding site is located at the base of this cleft and binds ADP, ADP+Pi or ATP complexed with a metal ion (Mg^{2+} or Ca^{2+}). As will be described later, in low salt solutions, actin molecules are present as monomers but in physiological salt solutions, actin monomers polymerize and form two-stranded helical filaments.

POLYMERIZATION OF ACTIN

Polymerization process of actin has been investigated in detail *in vitro*. Polymerization occurs only above a certain concentration (critical concentration), and can be regarded as a condensation process, much the same way as salt crystals grow in solution above a critical concentration (Kasai et al., 1962). In vitro polymerization has been shown to proceed in three steps, the nucleation step, the elongation step when actin monomers polymerize one after the other to the ends of polymerizing filaments, and the steady state when dissociation and polymerization of actin monomer are balanced in dynamic equilibrium (Fig. 2). In the first nucleation phase,

three actin monomers form an unstable trimer that serves as a polymerization nucleus (Pollard, 2007). Nucleation phase is rate-limiting in actin polymerization under certain in vitro conditions. In the subsequent elongation phase, elongations occur by addition of actin monomers to both ends of the growing filaments (Bonder et al., 1983). Elongation rates at each end of the filament are different (Kondo and Ishiwata, 1976; Woodrum et al., 1975), and the faster growing end is called the "plus" end or "barbed"-end, owing to the characteristic binding orientation of myosin S1 along the filament. In contrast, the slower growing end is called the "minus" end or "pointed"-end. When the concentration of free actin monomers decreases to the critical concentration, polymerization stage enters the steady state. In this steady state, elongation of actin filaments are observed only at the barbed end, which is balanced by the loss of actin monomers from filaments at the pointed-end. This process is called treadmilling (Wegner, 1976). When treadmilling occurs the concentration of actin monomers in solution is maintained at a critical concentration (~0.2 μM depending on the condition) (reviewed by Carlier, (1990)). Due to the hydrolysis of bound nucleotide, structures of actin subunits at both ends are different, and the barbed-end is more stable than the pointed-end (discussed later). Accordingly, the critical concentrations at both ends of actin filaments are also different, and it is ~0.12 μM at the barbed-end and ~0.6 μM at the pointed-end (Carlier, 1990). This difference of critical concentrations at both ends drives treadmilling.

Actin monomer hydrolyzes bound ATP very slowly, and therefore, most of actin monomer carries ATP. After actin monomers polymerize, bound ATP is hydrolyzed to ADP-Pi. The resulting Pi is slowly released from actin subunits in filaments, so that older actin subunits in filaments carry ADP. Therefore, actin subunits near the barbed-ends carry either ATP or ADP-Pi, while those near the pointed-ends have bound ADP. Actin subunits with bound ATP or ADP-Pi stabilize the filament structure, while those with bound ADP destabilize the filaments (reviewed by Korn et al., (1987)). This nucleotide-dependent difference in filament stability is the molecular basis for the asymmetric ends of an actin filament in the steady state.

COFILIN

Cofilin was identified as a protein involved in the depolymerization of actin filaments (Nishida et al., 1984). Cofilin, together with ADF (actin depolymerizing factor), forms a family of proteins with a molecular mass of 15,000-20,000, and is present in various eukaryotic cells, including plants, fungi and animals. It is an essential protein for growth of yeast (Iida et al., 1993; Moon et al., 1993) and the cellular slime molds (Aizawa et al., 1995). In human, there are three isoforms; muscle cofilin, non-muscle cofilin and ADF (Ono, 2007). It is necessary for the development of skeletal muscle (Miyauchi-Nomura et al., 2012) and maintenance (Agrawal et al., 2012).

Cofilin is able to bind to both actin monomer and filaments. After cofilin binds to actin filaments, twist of the filament increases (Galkin et al., 2001; McGough et al., 1997), and it is suggested that the resultant strain in the filament is correlated with the filament severing activity of cofilin (De La Cruz, 2009). Affinity of plant ADF and *Acanthamoeba* actophorin are higher for ADP-bound than for ATP-bound actin subunits in filaments, and for this reason, cofilin is believed to play an important role in the turnover of the actin cytoskeleton by selectively severing older sections of the filaments. Hotulainen et al. estimated that most of the cellular actin cytoskeleton is turned over by cofilin, and therefore, unveiling how cofilin interacts with actin filaments and how the process is regulated are critically important to understand the mechanism of actin regulation.

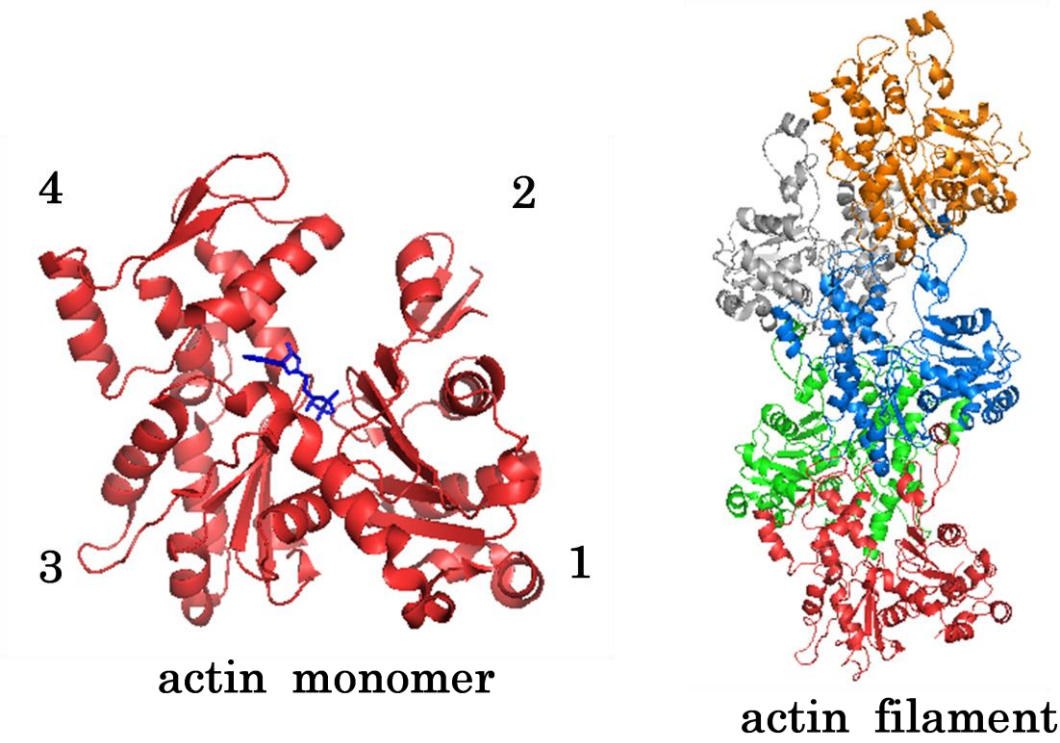

Figure 1. Structures of an actin monomer and an actin filament. Left; Crystal structure of monomeric actin in the ATP state (PDB ID: 1NWK; Graceffa and Dominguez, 2003) is represented in ribbon model (red). The ATP molecule is shown as a stick model (blue). The numbers indicate subdomains. Right; Cryo-EM structure of an actin filament in the presence of phosphate (PDB ID: 3G37; Murakami et al., 2010) is edited to contain 5 actin subunits. Each actin subunit is displayed in a different color.

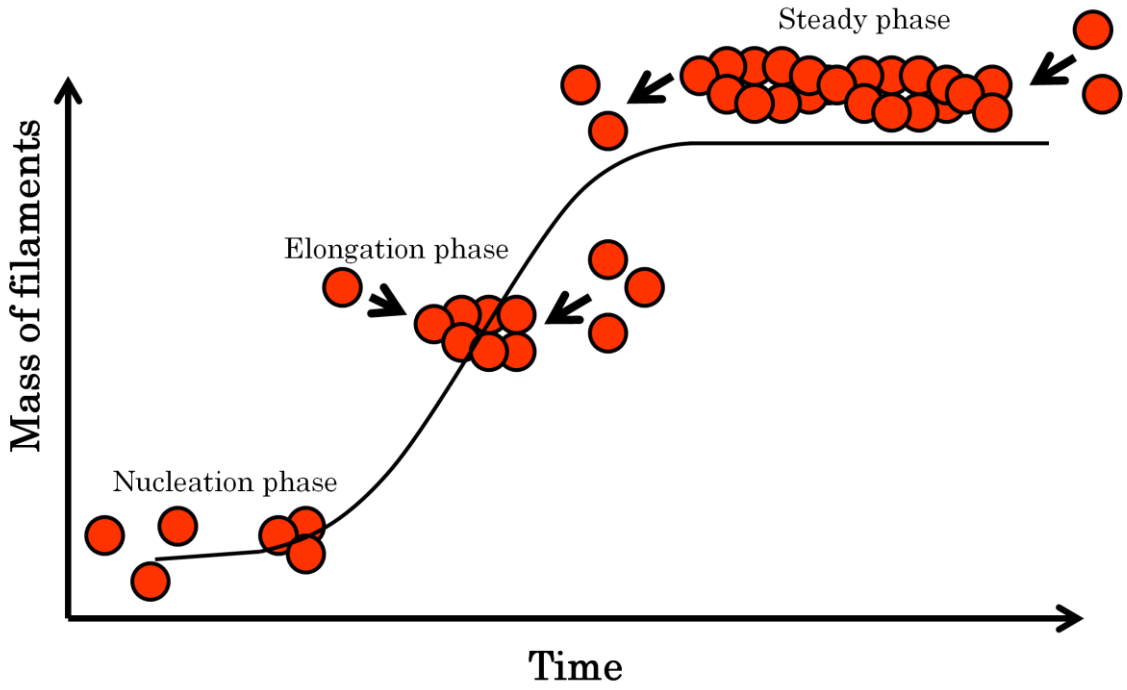

Figure 2. Three phases of actin polymerization. In the nucleation phase, three actin monomers slowly associate to make an unstable trimer complex. The trimer serves as the nucleus for polymerization. The rate of nuclei formation is determined by the concentration of actin monomers. In the elongation phase, actin monomers bind to both ends of the growing filaments. In the steady state, actin monomers only bind to the barbed-ends, which is balanced by dissociation of actin monomers from the pointed-ends. Treadmilling occurs in this phase.

Chapter I

Effects of bound nucleotide on the affinity of actin for cofilin

INTORODUCTION

A large number of cellular activities involve actin filaments, and this requires that polymerization and depolymerization of actin filaments are appropriately controlled spatially and temporally. Actin itself has the potential to polymerize and depolymerize depending on the solution conditions, but the cellular concentration of actin is much higher than the critical concentration for polymerization and most of the actin molecules would be stably polymerized in the solution condition of the cytoplasm. Thus, cells contain various actin binding proteins to regulate polymerization and depolymerization of actin filaments (Pollard et al., 2000). For example, cofilin is known to regulate polymerization and reorganization of actin filaments at the actin patch in yeast cells (Lappalainen and Drubin, 1997). Further, cytoskeletal dynamics, which is critical for motility of mammalian cells, depend on a pool of actin monomers that was maintained by the activity of ADF/cofilin (Hotulainen et al., 2005).

Cofilin is an actin-binding protein that binds to both the filamentous and monomeric actin, or F-actin and G-actin respectively. Cofilin bound to actin monomer is believed to prevent its polymerization by inhibiting the exchange of bound ADP to ATP (Hawkins et al., 1993; Hayden et al., 1993). On the other hand, cofilin that is bound to a filament accelerates depolymerization by severing the filament. To support continuous cell movement, cofilin needs to bind to and promote disassembly of older filaments at the back of a lamellipodium, while not affecting newly polymerized filaments at the leading edge of the lamellipodium. It is generally explained that this is achieved by asymmetric distribution of bound nucleotides in actin filaments, as follows. Polymerization of an ATP-actin monomer stimulates hydrolysis of bound ATP to ADP-Pi (Wegner, 1977). Pi is then slowly released, and ADP-actin is eventually formed. Because incorporation of actin monomers to filaments occurs primarily at the barbed ends in cells, older ADP-actin subunits are accumulated near the pointed ends of filaments. Carlier et al. (1997) and Blanchoin and Pollard (1999) showed by biochemical assays that plant cofilin and *Ancathamoeba* actophorin, both members of the ADF/cofilin family, prefer to bind to actin with bound ADP. Thus, if mammalian cofilin also prefers to bind ADP-actin, this would bias binding of cofilin to older ADP-actin subunits near the

pointed ends of filaments.

Electron microscopy study (Galkin et al., 2001), as well as classic solution binding assays (Hawkins et al., 1993; Hayden et al., 1993), demonstrated that cofilin binds cooperatively to actin filaments, and this phenomenon may be related to differential distribution of nucleotide states within filaments. In the anterior region of migrating amoeba cells of *Dictyostelium discoideum*, for example, dendric network of actin filaments polymerized by the activity of Arp2 / 3 is disassembled by cofilin (Aizawa et al., 1997). On the other hand, myosin II is enriched in the posterior region and drives the detachment of that portion of the cell from the substrate and retraction (Tsujioka et al., 2012; Yumura et al., 1984). Therefore, I speculated that the differential distribution of nucleotide states of actin subunits is correlated with multiple different structures of actin filaments, and that this polymorphism of actin filaments plays an important role in localizing different actin binding proteins at different sites within cells.

In view of the above, I thought that it is important to examine in detail the differential affinity of cofilin for actin filaments with different bound nucleotides. For this purpose, I first labeled human cofilin and skeletal actin with fluorescent dyes of different fluorescence spectra. As a source of cofilin, I used human cofilin since previous studies to show cofilin's preference to bind ADP-actin used either plant (Carlier et al., 1997) or *Acanthamoeba* (Blanchoin and Pollard, 1999) ADF/cofilin protein. I then observed binding of various concentrations of cofilin to actin filaments prepared under different nucleotide conditions using a fluorescence microscope.

EXPERIMENTAL PROCEDURES

Purification of Cofilin-mCherry

DNA of mCherry (Shu et al., 2006) was amplified by PCR using two primers. After confirmation of the sequence, the DNA fragment was inserted at the *Bam*HI and *Xba*I sites of pCold I (Takara Bio, Otsu, Japan) carrying a human cofilin gene (kindly provided by Dr. A. Nagasaki). The resultant plasmid was used to transform Rosetta (DE3) *E. coli* cells (Novagen). The transformed cells were inoculated in 100 ml of LB medium supplemented with 10 μg/ml chloramphenicol and 50 μg/mL ampicillin, and were shaken vigorously at 37℃ until the absorbance at 600 nm reached 0.5. After incubation for 30 min at 15℃, the culture was supplemented with 0.5 mM isopropyl-thiogalactopyranoside (IPTG) and shaken overnight at 16℃.

The *E. coli* cells were collected by centrifugation, and were frozen at -80℃. The pellets were suspended in 5 ml Lysis Buffer (100 mM NaCl, 10 mM 4-(2-hydroxyethyl)-1-piperazineethanesulfonic acid) (HEPES), pH 7.5) containing 0.1% Triton X-100. After sonication on ice using a Branson Sonifier (Model GE-60), this solution was clarified by centrifugation (15,000 rpm for 15 min at 4℃). The supernatant was supplemented with 10 mM imidazole (pH 7.4) and incubated with 2 ml of Ni-NTA agarose resin (Qiagen) on a rotary wheel for 1 hr at 5℃. The resin was recovered by a brief centrifugation at 1,000 rpm and was suspended in 15 ml Lysis Buffer that contained 30 mM imidazole. This procedure was repeated three times, and finally the resin was suspended in 2 ml Lysis Buffer containing 500 mM imidazole. The suspension was clarified by centrifugation, and the supernatant was dialyzed overnight against Lysis Buffer. The purity was checked by SDS-PAGE (Fig. 3).

Fluorescence labeling of actin by Alexa-488

Fluorescence labeling of actin by Alexa 488 was carried out according to the method of Fujiwara et al. (2007). First, skeletal muscle actin, prepared by the method of Spudich and Watt (1971), was polymerized while being dialyzed against buffer (50 mM piperazine-1,4-bis(2-ethanesulfonic acid) (PIPES) (pH 6.8), 100 mM KCl, 0.2 mM ATP, 0.2 mM $MgCl_2$). After being diluted to 2 mg/ml in the same buffer, F-actin was reacted overnight by adding 7.39 μM Alexa-Fluor 488 succinimidyl ester (Invitrogen, Tokyo,

Japan) from a stock solution of 60 mM in *N,N*-dimethylformamide. The labeled F-actin was pelleted by ultracentrifugation at 75,000 rpm for 15 min at 4℃ (Hitachi CS-100GX Ultracentrifuge), dissolved in G-buffer (0.2 mM ATP, 0.2 mM $CaCl_2$, 0.5 mM dithiothreitol (DTT), and 2 mM Tris, pH 8.0) and dialyzed overnight against G-buffer. Actin fluorescently labeled was 61% of the total.

AMP-PNP actin

ATP and DTT in a solution of 40 μM Alexa 488 actin in G-buffer were removed using ion-exchange resin (Strzelecka-Golaszewska, 1973). First, Dowex-1 (bed volume ~ 1 ml) in a spin column was equilibrated with G-buffer without DTT and ATP. A 70 μl solution of 40 μM Alexa 488 actin was loaded to the column, and the actin solution was recovered by centrifugation (800 ×g, for 2 min). After addition of adenosine 5′-(β,γ-imido)triphosphate (AMP-PNP) to a concentration of 0.2 mM, the solution was incubated overnight on ice.

Fluorescence microscope observation

Three types of actin with bound ADP, ADP-Pi or AMP-PNP were polymerized as follows.
ADP-actin: Alexa 488-actin was polymerized at 4 μM for 2 hr at 25℃ in Mg-buffer (25 mM imidazole, pH 6.5, 4 mM $MgCl_2$, 25 mM KCl, 1 mM DTT).
ADP-Pi-actin: After 2 hr of polymerization of Alexa 488-actin in Mg-buffer as above, 10 mM Na-phosphate (pH 7.4) was added and incubated for 2 hr.
AMP-PNP-actin: Alexa 488-actin incubated with AMP-PNP as above was polymerized for 2 hr in Mg-buffer at the final concentration of 4 μM.

Each type of actin filaments was diluted in Mg-buffer containing cofilin-mCherry, so that the final concentrations of Alexa-actin and cofilin-mCherry were 40 nM and 200, 400, 600, 800 or 1,600 nM, respectively. After 2 min incubation, approximately 2 μl of these solutions was placed between a glass slide and a coverslip, and was observed within 2 min using a fluorescence microscope (ECLIPS E600, Nikon) equipped with a highly sensitive CCD camera (ARUGUS-HiSCA, Hamamatsu Photonics).

RESULTS

Figures 4 to 6 are fluorescence micrographs showing binding of 400, 600, 800 or 1,600 nM cofilin-mCherry to Alexa 488-actin filaments. Note that Alexa 488 fluorescence is suppressed when the Alexa 488-actin filaments were bound with cofilin-mCherry. This is not due to fluorescence resonance energy transfer (FRET), since in bulk measurements of fluorescence intensity, mixing of Alexa 488-actin and cofilin-mCherry decreased the fluorescence intensity of Alexa, but the fluorescence intensity of mCherry did not rise (N. Umeki, unpublished observation).

When ADP-bound (Fig. 4) and AMP-PNP-bound (Fig. 6) actin filaments were used, only weak fluorescence of cofilin-mCherry could be detected along small number of filaments in 400 nM cofilin-mCherry. At 600 nM cofilin-mCherry, stronger fluorescence of cofilin-mCherry could be detected along larger number of actin filaments. When the concentration of cofilin-mCherry reached 800 nM, approximately 80% of the filaments were bound with cofilin-mCherry. In the presence of 1,600 nM cofilin-mCherry, the fluorescence patterns were similar to those in the presence of 800 nM, but the observation became difficult due to high background fluorescence of cofilin-mCherry. In contrast, when ADP-bound actin filaments were incubated with cofilin-mCherry in the presence of 10 mM Pi, fluorescence of cofilin-mCherry could be hardly detected along the filaments, even at the highest concentration (1,600 nM) of cofilin-mCherry tested (Fig. 5).

Figure 7 summarizes the percentage of actin filaments with bound cofilin-mCherry, made by visual counting of filament images in Alexa 488 and mCherry fluorescence channels. Again it is evident from this graph that the affinity of ADP-Pi-bound actin filaments for cofilin is much lower compared to the other two forms of actin filaments.

Intriguingly, in the presence of 800 or 1,600 nM cofilin-mCherry, there appears to be two distinct intensities of mCherry along ADP- or AMP-PNP-bound filaments. Figure 8 is a representative fluorescence micrograph demonstrating this point.

DISCUSSION

Effects of the nucleotide state of actin filaments on affinity for human cofilin

The results shown in Figures 4 and 6 demonstrated that, when present at 600 nM or above under the current experimental conditions, human cofilin-mCherry binds to actin filaments carrying ADP or those incubated with AMP-PNP. In contrast, in the presence of 10 mM Pi, very little cofilin-mCherry was observed to bind ADP-bound actin filaments even at the highest concentration of cofilin-mCherry tested (Fig. 5). Under this condition, most of the ADP-bound actin subunits in filaments presumably bound Pi, since Kd of ADP-actin for Pi is approximately 1.5 mM (Carlier and Pantaloni, 1988); several fold lower than the concentration of Pi in the solution. Therefore, I interpreted this result to mean that human cofilin has very low affinity for actin subunits carrying ADP-Pi, consistent with the previous reports that used either plant (Carlier et al., 1997) or *Acanthamoeba* (Blanchoin and Pollard, 1999) ADF/cofilin protein. In cells, including mammalian cells, it is speculated that cofilin plays important role in remodeling of the actin cytoskeleton by selectively binding and severing older actin filaments (Pollard et al., 2000). It is generally believed that this cofilin's preference to sever older filaments is based on preferential binding of cofilin to actin subunits carrying ADP, over those carrying ADP and Pi. This is because, in the cytoplasm, in which Pi concentration is ~ 2 mM (Burt et al., 1977), Pi is slowly released from actin subunits carrying ADP and Pi.

AMP-PNP is a commonly used non-hydrolyzable analog of ATP (Yount et al., 1971), and therefore, if AMP-PNP is bound at the ATP binding site of actin, that actin molecule is expected to stay in the ATP-bound state. If those AMP-PNP-bound actin monomers polymerize, the entire filament is expected to mimic the ATP-bound state. It was therefore surprising that cofilin-mCherry bound to filaments incubated with AMP-PNP as well as to those carrying ADP (Fig. 6). Since AMP-PNP is not a faithful mimic of ATP, it is possible that actin subunits with bound AMP-PNP actually behaved like an ADP-bound form. However, a more likely explanation is that AMP-PNP was released from actin subunits during incubation with cofilin-mCherry, since 40 μM Alexa 488-actin solution containing 0.2 mM AMP-PNP was diluted 10-fold in the reaction mixture so that the concentration of AMP-PNP in the reaction mixture was 20 μM, which is roughly the same as the Kd of

actin for AMP-PNP (Cooke, 1975). Furthermore, binding of cofilin might accelerate or promote the release of bound AMP-PNP in a cooperative manner, as it does to Pi that is bound to actin filaments (Suarez et al., 2011). To distinguish between these two possibilities, it would be necessary to repeat the experiment in the presence of a high concentration of AMP-PNP in the reaction mixture.

Cooperative binding

In this study, I was able to observe cooperative binding of human cofilin to actin filaments by fluorescence microscopy. Cooperative binding of cofilin to actin filaments was first suggested by solution binding experiments in which the fraction of actin-bound cofilin showed a sigmoidal dependence on the cofilin concentration (Hawkins et al., 1993; Hayden et al., 1993). More recently, cooperative binding of cofilin to actin filaments was directly observed by electron microscopy (Galkin et al., 2001). Cofilin forms dense clusters along actin filaments, while leaving other parts of the filament unbound. The present study extended this finding and showed that the cooperative binding occurs in a range of micrometers along actin filaments. Recently, a similar fluorescence microscopic study using yeast cofilin was published (Suarez et al., 2011), and Suarez et al.'s results are largely consistent with my results presented here.

Intriguingly, it appears that there are two types of cooperative binding between human cofilin and actin filaments, weak and strong, as shown in Figure 8. The simplest interpretation of this phenomenon is that there are two densities of cofilin molecules in clusters; in the "weak" cooperativity, cofilin binds sparsely in clusters, and in the "strong" cooperativity, cofilin binds at full density (1:1 molar ratio with respect to actin subunits) in the clusters. Because Suarez et al. (2011) did not mention such two different modes of cooperative binding, this may be specific to human cofilin or to some subtle differences in our experimental conditions. However, it is possible that the brighter portion may represent bundling of filaments, since in the presence of high concentration of cofilin, a larger number of severed filament fragments are produced, and those filament fragments may associate with one another while in solution. To exclude this possibility, I tried to improve the observation method by first immobilizing actin filaments to the glass surface lightly coated with

poly-lysine and then applying a solution of cofilin-mCherry. However, the poly-lysine treatment absorbed high concentration of cofilin-mCherry to the surface, which increased the background fluorescence and hindered the observation. Further, since the binding of cofilin increases the twist of actin filaments (McGough et al., 1999), it is feared that immobilization of actin filaments might inhibit cofilin binding by restricting the twisting motion of the bound filaments. It is therefore a challenge for the future improvement to design an experimental system that allows observation of binding of fluorescent human cofilin to actin filaments loosely immobilized on a surface.

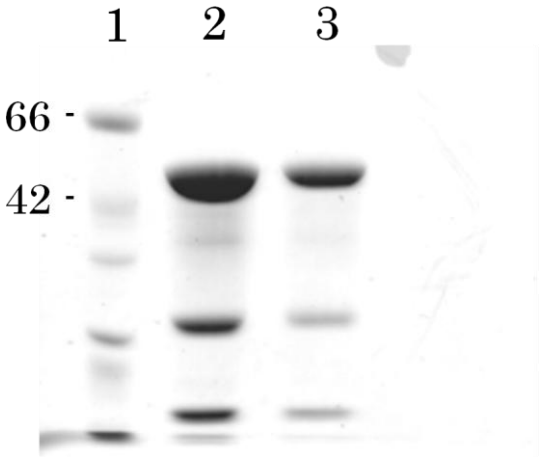

Figure 3. SDS-PAGE of cofilin-mCherry. Lane 1 is the molecular weight markers. Lanes 2 and 3 show two different batches of purified cofilin-mCherry. The top bands in these lanes are cofilin-mCherry (deduced molecular weight = 48,598).

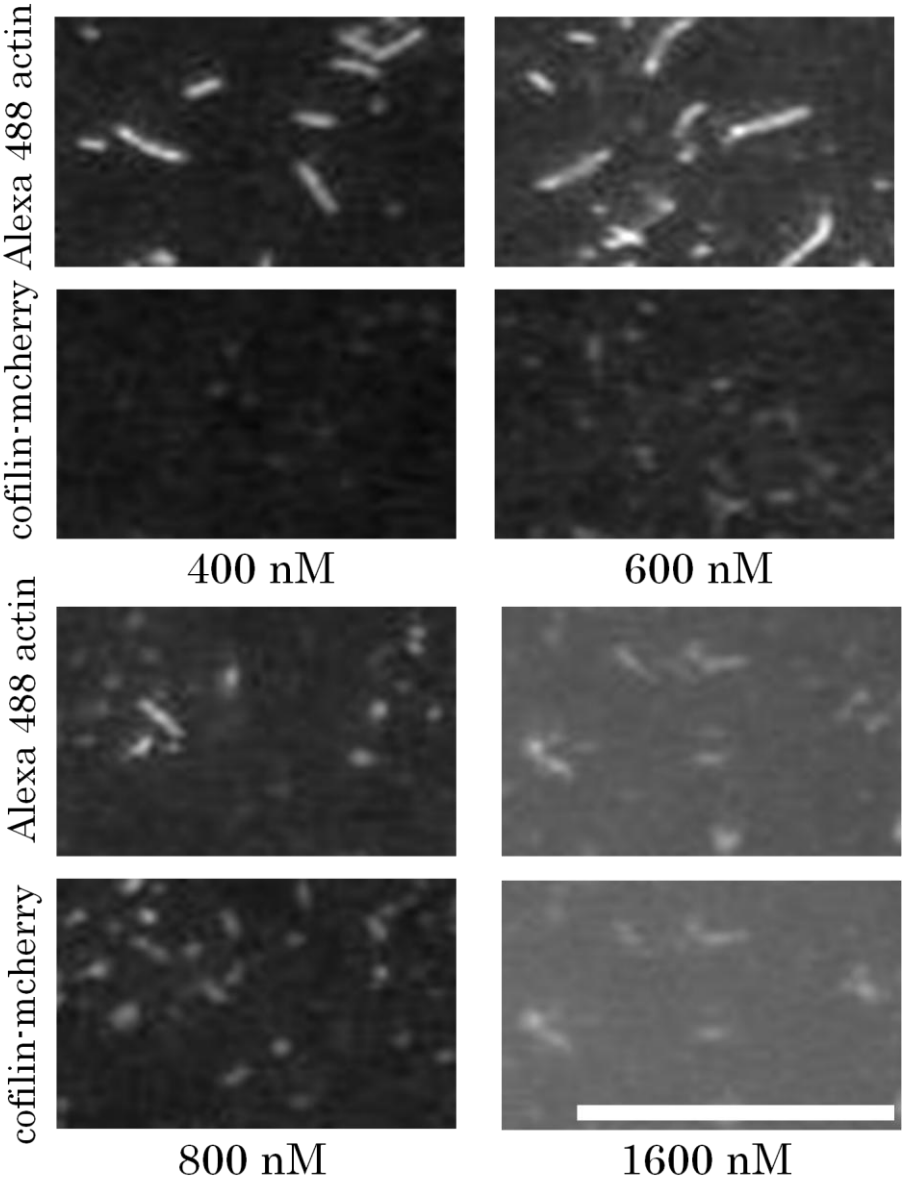

Figure 4. Binding of cofilin-mCherry to actin filaments with bound ADP. Upper and lower images of each column are Alexa 488 and mCherry fluorescence micrographs of the same field, respectively. In the presence of 400 nM cofilin-mCherry, binding of cofilin-mCherry to actin filaments was barely detectable. Some actin filaments were bound with cofilin-mCherry at 600 nM, and binding intensity increased when the concentration of cofilin-mCherry was further raised. Alexa and mCherry fluorescence micrographs were taken and processed under the same condition, respectively, so that the fluorescence intensities can be compared within each row. Scale bar, 10 μm.

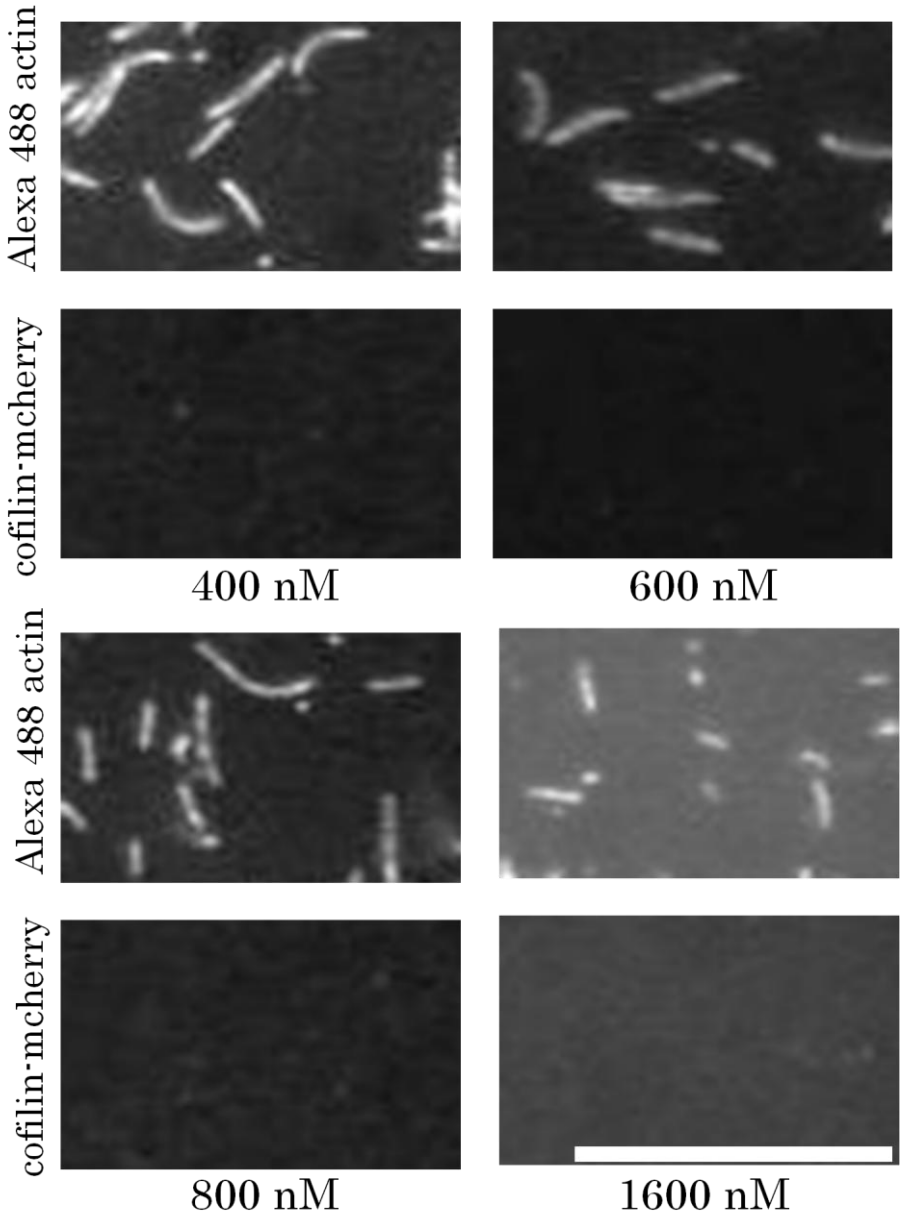

Figure 5. Binding of cofilin-mCherry to actin filaments with bound ADP in the presence of 10 mM Pi. Upper and lower images of each column are Alexa 488 and mCherry fluorescence micrographs of the same field, respectively. Practically no binding of cofilin-mCherry to actin filaments was detected at all concentrations of cofilin-mCherry tested. Scale bar, 10 μm.

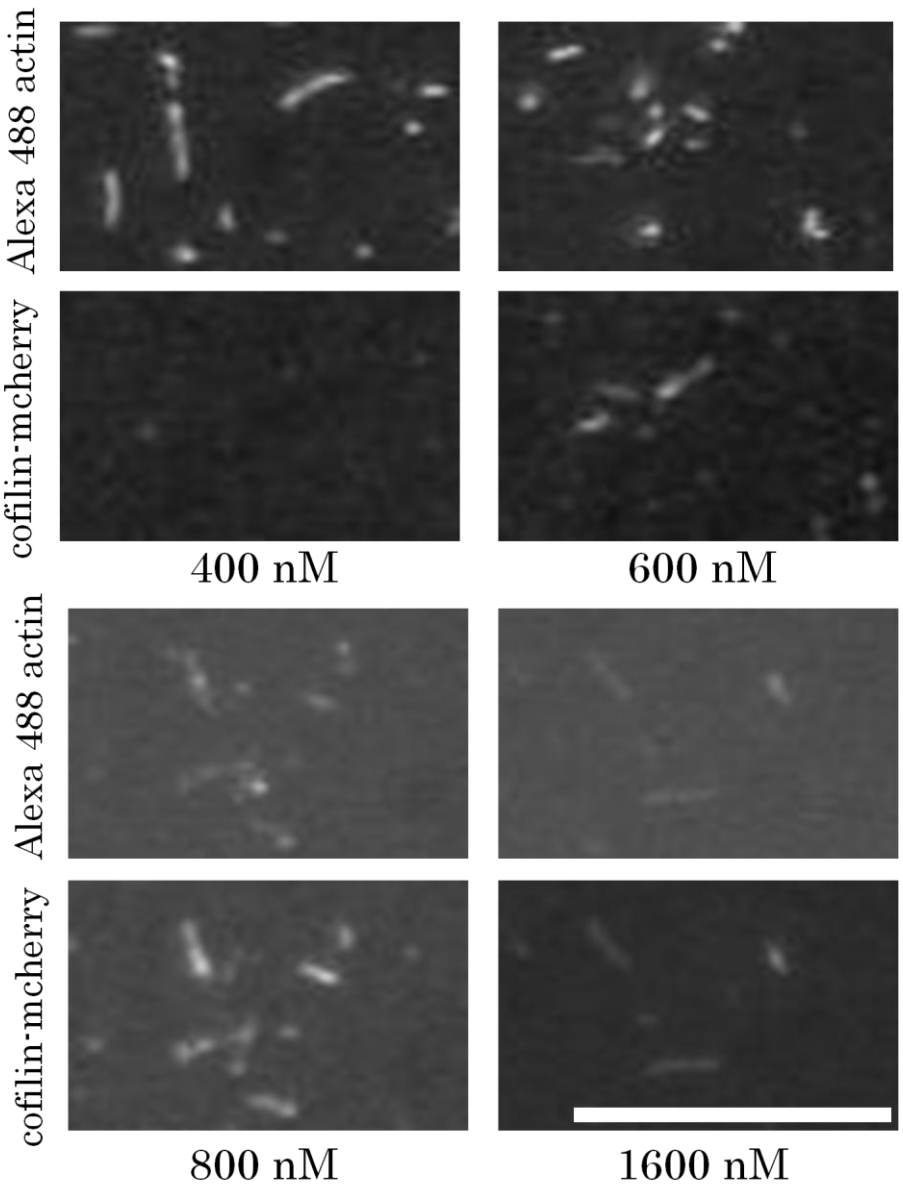

Figure 6. Binding of cofilin-mCherry to actin filaments incubated with AMP-PNP. Upper and lower images of each column are Alexa 488 and mCherry fluorescence micrographs of the same field, respectively. In the presence of 400 nM cofilin-mCherry, binding of cofilin-mCherry to actin filaments was barely detectable. Some actin filaments were bound with cofilin-mCherry at 600 nM, and binding intensity increased when the concentration of cofilin-mCherry was further raised. Alexa and mCherry fluorescence micrographs were taken and processed under the same condition, respectively, so that the fluorescence intensities can be compared within each row. Scale bar, 10 μm.

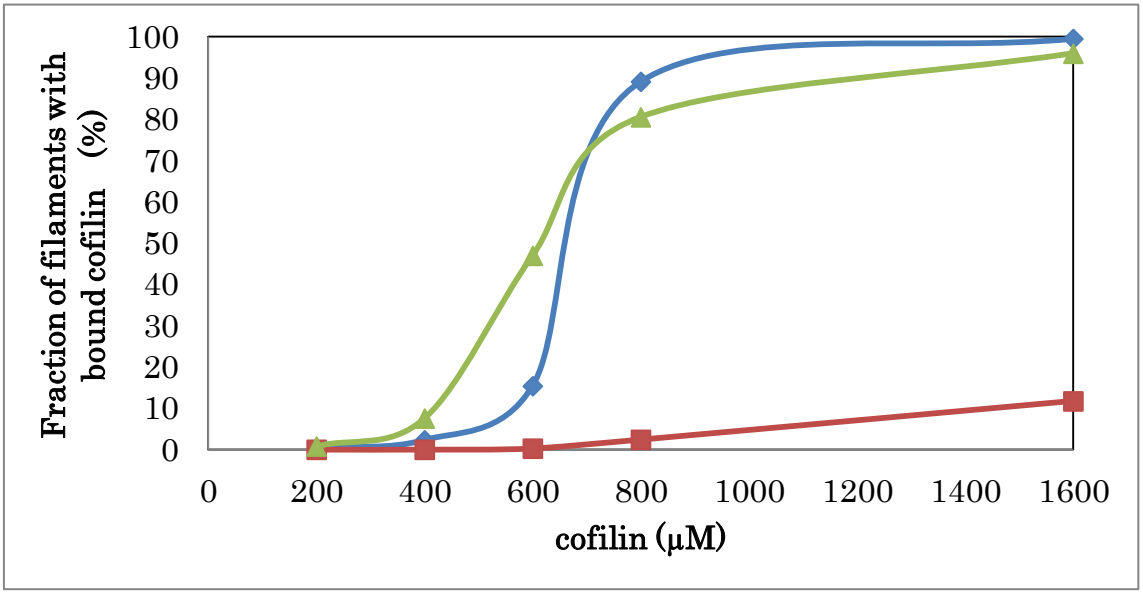

Figure 7. Percentage of actin filaments with bound cofilin-mCherry. For each determination, three sets of fluorescence micrographs were used, and a total of more than 300 filaments were evaluated. Filaments with local binding were counted as bound, but small dot-like objects were not counted. In the case of filaments with bound ADP (a blue line with diamond symbols), fraction of bound filaments rose sharply between cofilin-mCherry concentration of 600 nM and 800 nM, and reached 90% at 800 nM. A similar tendency was observed in the case of filaments incubated with AMP-PNP (a green line with triangle symbols), but the slope appeared shallower than in the case of ADP-bound filaments. In the presence of 10 mM Pi (a red line with square symbols), there were only 10 % of bound actin filaments even at 1,600 nM cofilin-mCherry. This is in sharp contrast to the other two types of actin filaments.

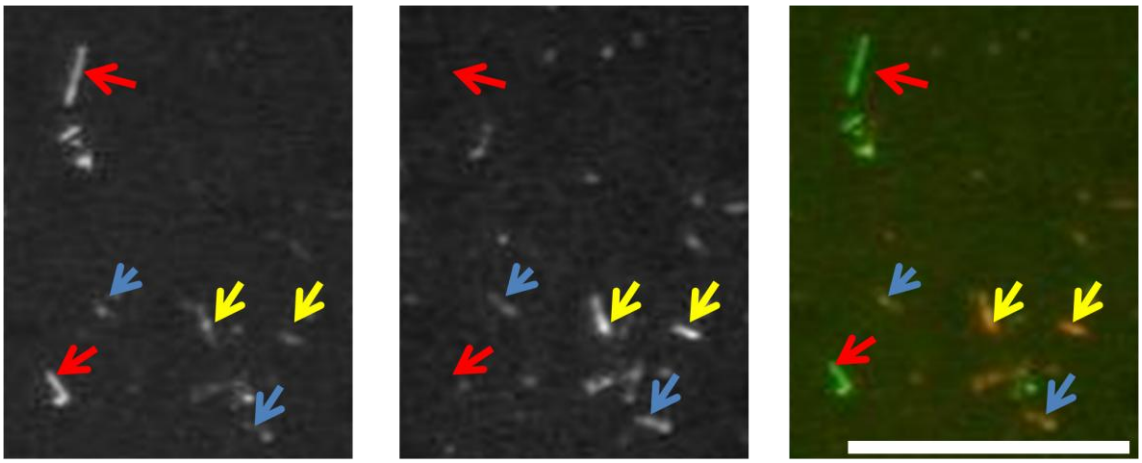

Figure 8. Two distinct intensities of cofilin-mCherry binding along actin filaments. Shown here as an example is a set of fluorescence micrographs demonstrating binding of 600 nM cofilin-mCherry (middle) to ADP-bound Alexa 488-actin filaments (left). The right is a merged image, with Alexa 488 fluorescence shown in green and mCherry in red. Actin filaments indicated by red arrows are not bound with cofilin-mCherry. Those indicated by blue arrows have bound cofilin-mCherry at a moderate intensity. Those indicated by yellow arrows have much higher mCherry fluorescence than those indicated by blue arrows. Scale bar, 10 μm.

Chapter Ⅱ

Characterization of Dominant Negative Asp11 Mutant Actins

INTORODUCTION

A variety of mutant proteins have proven useful for elucidating the molecular mechanisms underlying protein functionality, and dominant negative mutants often provide unique opportunities in such studies. In that regard, a large number of actin mutations, some of which are dominant negative, have been identified through experimental genetic screening (An and Mogami, 1996; Drummond et al., 1991; Noguchi et al., 2010a; Wertman et al., 1992) and analysis of human hereditary diseases (e.g., Laing et al., 2009; Monserrat et al., 2007; Morita et al., 2008; Olson et al., 1998; van Wijk et al., 2003; Zhu et al., 2003). Unfortunately, however, recombinant actin must be expressed in eukaryotic host cells (Sternlicht et al., 1993), and expression of dominant negative actin mutants is toxic to the cells, which has hampered the mutants' biochemical characterization (Wertman et al., 1992). To overcome this limitation, Noguchi et al. (2007) developed a system for expressing toxic mutant actins in *Dictyostelium*. With this system, thymosin β is fused to the C-terminal of the mutant actin to block its copolymerization with the endogenous actin. The fusion protein is then purified and treated with chymotrypsin, which efficiently cleaves the protein immediately after the final native actin residue, separating the actin and thymosin moieties (Noguchi et al., 2007). This expression system was used to characterize dominant negative actin mutations (Noguchi et al., 2010b) previously identified in *Drosophila* indirect flight muscle (An and Mogami, 1996), as well as in a genetic screens using yeast cells (Noguchi et al., 2010a). These studies demonstrated the usefulness of dominant negative mutant actins and prompted me to characterize other dominant negative actin mutants.

Within the budding yeast actin sequence, Asp 11 is a component of the nucleotide-binding site (Fig. 9) and is conserved among all known actins. The D11Q yeast actin mutant (D13Q in α actin and D12Q in the *Dictyostelium* actin 15; the yeast amino acid residue number will be used throughout this chapter) was found to bind DNase I only poorly (Solomon et al., 1988), and its overexpression in yeast cells demonstrated it to be dominantly lethal (Johannes and Gallwitz, 1991), making its purification for detailed biochemical characterization difficult. More recently, a D11N mutation in human α actin was shown to dominantly cause congenital

myopathy (Laing et al., 2009), further highlighting the need to characterize Asp11 mutant actins in vitro. I therefore constructed *Dictyostelium* versions of the D11N and D11Q mutant actins, purified them using the thymosin-fusion system, and characterized them in various biochemical assays. The results demonstrate that D11N/Q actin polymers are abnormal in several ways: they are slow to polymerize to form filaments and are similarly slow to depolymerize, and their binding to cofilin is defective. The monomeric forms also exhibit abnormalities, including defective cofilin binding and resistance to subtilisin cleavage at the DNase binding loop. Most notably, copolymers of D11N/Q and WT actins exhibit partial resistance to cofilin-mediated acceleration of depolymerization. The failure of copolymerization with WT actin to fully correct the defective cofilin-induced depolymerization of D11N/Q actins suggests that defective cofilin binding is the primary reason why D11N/Q actins are dominantly toxic in yeast and human.

EXPERIMENTAL PROCEDURES

Plasmid construction

pTIKL ART (Noguchi et al., 2007) contains an *ART* gene, which is the *Dictyostelium act15* gene modified to carry four unique restriction sites (the AR gene), followed by a Gly-based linker, a synthetic human thymosin β gene and a His tag. pTIKL GFP-AR carries a GFP-fused AR gene (Noguchi et al., 2007). D11N and D11Q mutations were made using a PCR-based method, and the mutant genes were subcloned into pTIKL ART and pTIKL GFP-AR after confirmation by DNA sequencing. The mutated sequences were GCTTTAGTTATTAATAACGGTTCTG and GCTTTAGTTATTCAAAACGGTTCTG for D11N and D11Q, respectively (the underlines show the mutated residues).

Cell culture

Dictyostelium discoideum Ax2 or KAX3 cells were transfected with pTIKL-based plasmids by electroporation (Egelhoff et al., 1991). Transfectants were then selected on plates at 21-22°C in HL5 medium containing 60 μg/ml each of penicillin and streptomycin and 12 μg/ml G418. For biochemical purification of actin, KAX3 cells expressing either WT or mutant ART were grown on plates in medium containing 40 μg/ml G418; large-scale cultures were grown first in 25 x 25 cm^2 plastic plates or 5 L conical flasks, and then in fresh HL5 medium containing 10 μg/ml G418 for an additional 24-36 h on a shaker.

Observation of GFP-mutant actin in live *Dictyostelium* cells

Ax2 cells expressing GFP-actin or its derivative were observed using a confocal laser scanning microscope (CSU-10, Yokogawa) (Noguchi et al., 2007)

Purification of actin and cofilin

Recombinant WT and mutant actins were purified as described previously (Noguchi et al., 2010b). Actin concentrations were estimated using an Advanced Protein Assay (Cytoskeleton, Denver, CO). Actin calibrated based on absorption at 290 nm served as the standard.

Dictyostelium cofilin cDNA (*Ddcof1*) (Aizawa et al., 1995) was isolated from a cDNA library using the primers 5'-GGTACCATGTCTTCAGGTATTGCT and 5'-CAATTGGATTTTGGTACATTTTTCAT and, after sequence verification, was inserted at the *Bam*HI and *Eco*RI sites of pCold I (Takara Bio, Otsu, Japan) or pCold I carrying a mCherry gene inserted at the *Eco*RI and *Xba*I sites. These were used to express N-terminally His-tagged cofilin or cofilin-mCherry in *E. coli* Rosetta (DE3) cells. The proteins were then purified using conventional methods.

Polymerization assay

Monomeric WT or mutant actin was diluted in G-buffer (2 mM Hepes (pH 7.4), 0.2 mM $CaCl_2$, 0.1 mM ATP, 7 mM β-mercapthoethanol, 0.05% NaN_3) and incubated on ice for 10 min. Polymerization was induced by addition of concentrated F-buffer, after which increases in 360 nm light scatter were monitored at 22°C using a fluorescence spectrophotometer with a 100-μL cuvette. The final concentration of each component was 5 μM actin, 2 mM Hepes (pH 7.4), 100 mM KCl, 2.5 mM $MgCl_2$, 0.5 mM EGTA, 0.2 mM ATP and 0.2 mM DTT.

Depolymerization assays

WT or mutant actin or a 1:1 mixture of WT and mutant actins were allowed to polymerize in F-buffer for 2 h at room temperature. The total actin concentration was 5 μM. Latrunculin A (Wako, Osaka, Japan) or DMSO control was then added to a final concentration of 60 μM or 0.3%. After incubation for 10 min, the mixtures were centrifuged at 250,000 x *g* for 10 min at 20°C, and the supernatant and pellet fractions were subjected to SDS-PAGE. Alternatively, WT actin labeled with pyrene at Cys374 (Kouyama and Mihashi, 1981) was used, and the reduction in pyrene fluorescence was monitored using a fluorescence spectrophotometer with excitation and emission wavelengths of 365 nm and 407 nm, respectively.

For direct observation of the depolymerization of individual actin filaments, the filaments (10 μM) were labeled by incubation overnight on ice in buffer containing 200 μM Alexa-Fluor 488 succinimidyl ester (Invitrogen, Tokyo, Japan), 2 mM Hepes (pH 7.4), 50 mM KCl, 2.5 mM $MgCl_2$, 0.5 mM EGTA and 0.2 mM ATP. The reaction was stopped by addition of 0.1 M

Tris-Cl pH7.4. After removing unbound dye using ion exchange resin (Dowex, 1x80, 100-200 Mesh), the labeled actin was dialyzed against G-buffer. The labeled monomeric actin was then mixed with unlabeled WT or D11Q actin in G-buffer at a 1:1 ratio and polymerized in F-buffer for 2 h at room temperature, as above. Once polymerized, the actin was diluted in assay buffer (10 mM Hepes (pH 7.4), 25 mM KCl, 4 mM $MgCl_2$, 10 mM DTT and 0.5% bovine serum albumin) and introduced into flow cells coated with 25 μg/mL skeletal heavy meromyosin, where it was incubated for 2 min. The flow cells were then perfused with copious amounts of 10 mM Hepes (pH 7.4), 100 mM KCl, 2.5 mM $MgCl_2$, 0.5 mM EGTA, 0.1 mM ADP, 10 mM DTT and an oxygen scavenger system, after which the actin filaments were observed using a fluorescence microscope (BX60, Olympus, Tokyo, Japan) equipped with an EB-CCD camera (C7190, Hamamatsu Photonics, Hamamatsu, Japan) at 25°C.

Phosphate Release Assay

The time course of Pi release from polymerizing actin was measured by using an EnzChek phosphateassay kit (Invitrogen). Actin was polymerized at 10 μM, as described under "Polymerization Assay," in the presence of 2-amino-6-mercapto-7-methylpurine riboside and 1 unit/ml purine nucleoside phosphorylase, and the absorbance at 360 nm was monitored.

Stopped Flow Analyses

The rates of 1,N^6-ethenoadenosine 5 ε-triphosphate (ε-ATP) release from monomeric actin was measured at 25°C using a stopped flow system (SX18MV:Applied Photophysics, Leatherhead, UK). Actin filaments were dialyzed against G-buffer for 24 h, followed by second dialysis against G-buffer that contained 0.2 mM ε-ATP (Invitrogen) in place of ATP for 24 h (WT) or 48 h (mutants). This solution was rapidly mixed with an equal volume of G-buffer that contained 1 mM CaATP, and fluorescence excited by 360 nm light and passed through a 395-nm cutoff filter was monitored.

Cofilin-binding assay

WT or mutant actin or a 1:1 mixture of WT and mutant actins were allowed to polymerize for 2 h at room temperature in buffer containing 20

mM Pipes (pH 6.5), 50 mM KCl, 2.5 mM $MgCl_2$, 0.5 mM EGTA, 0.2 mM ATP and 0.2 mM DTT. Cofilin was then added to a final concentration of 2.5 μM, and 5 min later the mixture was centrifuged at 250,000 x *g* for 10 min at 20°C. The resultant supernatant and pellet fractions were subjected to SDS-PAGE.

For microscopic observation of cofilin binding to actin filaments, 1 μM Alexa 488-labeled actin filaments were mixed with 2 μM cofilin-mCherry in buffer comprising 10 mM Pipes (pH 6.5), 50 mM KCl, 1 mM $MgCl_2$, 5 mM DTT and 1 mM ATP. After incubation for 1 min at 25°C, the labeled actin filaments were diluted 10 fold in the same buffer, placed on a glass slide, overlaid with a coverslip, and observed using a fluorescence microscope.

Cofilin binding to monomeric actin was detected by crosslinking the proteins using 1-ethyl-3-(3-dimethylaminopropyl) carbodiimide (EDC; Sigma, St. Louis, MO). Mixtures of 7 μM actin and 14 μM cofilin in G-buffer were treated with 40 mM EDC for 5 min at 25°C. After stopping the reaction by addition of SDS sample buffer, the samples were analyzed by SDS-PAGE.

Cofilin-induced depolymerization assay

A 1:1 mixture of Alexa 488-labeled WT actin and unlabeled WT or D11Q actin was polymerized in F-buffer for 2 h at room temperature, as above. The final concentration of each actin was 2.5 μM. Hepes (pH 8.35) and cofilin were added to final concentrations of 10 mM and 10 μM, respectively, and 15 min later the mixture was centrifuged at 250,000 x *g* for 10 min at 25°C. The supernatant and pellet fractions were then subjected to SDS-PAGE and stained with Coomassie Blue. The gel was also viewed on a Molecular Dynamics Typhoon 8600 Imager (excitation wavelength: 532 nm; GE Healthcare, Little Chalfont, UK).

For microscopic observation of cofilin-induced severing/depolymerization of actin filaments, copolymers of Alexa 488-labeled WT actin and either unlabeled WT or D11Q actin were diluted to 40 nM in buffer containing 10 mM Hepes (pH 8.35), 30 mM KCl, 1 mM $MgCl_2$, 0.2 mM ATP, 5 mM DTT and 2 μM cofilin. After incubation for 5 min at 25°C, the mixture was observed using a fluorescence microscope.

Subtilisin cleavage assay

G-actin (5 μM) was digested with 1 μg/mL subtilisin (Sigma) at 25°C in modified G-buffer (2 mM Tris-Cl (pH 7.4), 0.2 mM $CaCl_2$, 0.2 mM ATP and 0.1 mM DTT). The reaction was then stopped by addition of 1 mM phenylmethylsulfonylfluoride, and the samples were analyzed by SDS-PAGE.

DNase I inhibition assay

DNase I activity was measured at 22°C based on changes in A_{260} of G-buffer containing 50 μg/mL DNA (Sigma), 0.7 nM DNase I (Sigma) and 10 nM G-actin.

Electron microscopy

WT or D11N/Q actin filaments in EM buffer (10 mM K-phosphate (pH 7.4), 25 mM KCl, 2.5 mM $MgCl_2$, 0.2 mM ATP and 0.5 mM DTT) were placed on carbon-coated copper grids, stained with 1% uranyl acetate, and observed using an FEI Tecnai F20 electron microscope.

RESULTS

Purification of D11N/Q actins

D11N and D11Q mutant actins were successfully expressed and purified as thymosin β fusion proteins with a polyhistidine tag. After separating the actin from the thymosin-his tag moieties through chymotryptic digestion, I was able to further purify the intact mutants using Q-Sepharose column chromatography followed by a cycle of polymerization, pelleting by ultracentrifugation, and dialysis against G-buffer.

Polymerization of D11N and D11Q actins

When monomeric D11Q actin in G-buffer was induced to polymerize by the addition of salts, the light scatter indicative of polymerization increased more slowly than with WT actin (Fig. 10A). Nonetheless, D11Q actin filaments visualized by rhodamine-phalloidin staining appeared to be normal (Fig. 10B). When a 1:1 mixture of WT and D11Q actins was allowed to polymerize, light scatter increased at an intermediate rate, between the rates for the WT and mutant homopolymers. I, with the help of Dr. K. Hirose, next used electron microscopy to observe negatively stained D11N/Q actin under polymerizing conditions, and were surprised to find that most of the D11Q/N polymers formed either small rings or short rod-like structures without a noticeable double-helical appearance; there were few filaments with a normal appearance (Fig. 11C, E). Addition of phalloidin did not noticeably increase the filamentous fraction of D11Q polymers (Fig. 11D). These results, together with the fact that the mutant actins were purified normally through a cycle of polymerization and depolymerization steps, indicate that D11N/Q actins are able to undergo salt-dependent reversible polymerization, but the polymerized products are mostly abnormal oligomeric structures.

When a 1:1 mixture of D11Q actin labeled with Alexa 594 and WT actin labeled with Alexa 488 were induced to polymerize and then observed under a fluorescence microscope, the same filaments could be visualized using either fluorophore (Fig. 12A). Interestingly, fluorescence intensities of both Alexa 488 and Alexa 594 were not homogeneous along the length of copolymers, suggesting the possibility that WT and D11Q actins tend to segregate from each other and form clusters. In addition, very bright

fluorescent dots of Alexa 594 were observed along the length (Fig 12A, arrowheads). This may represent oligomeric structures of D11Q actin associated along the sides of filaments, as seen in electron micrographs (arrowheads in Fig. 11C). When GFP-fused D11Q actin was expressed in *Dictyostelium* cells, the fluorescence was localized along cell edges, in thin projections and in macropinocytotic cups (Fig. 12B). This distribution was similar to that of GFP-WT actin (Fig. 12B), but distinctly differed from that of non-polymerizable GFP-WT actin fused at its C-terminal with thymosin β (Fig. 12B). The level of cytoplasmic GFP-D11Q actin fluorescence, which was derived from both monomeric and oligomeric GFP-actin, was low and comparable to that of GFP-WT actin, suggesting that GFP-D11Q and GFP-WT actins copolymerized with endogenous actin with similarly high efficiencies. Western blotting analysis (Fig. 12C) showed that 53 ± 15% of GFP-WT actin was recovered in the Triton-insoluble fraction, whereas 30 ± 2.3% of GFP-D11Q actin was in the insoluble fraction (N=3; the insoluble fraction of GFP-D11Q actin fused with thymosin β was 7.0 ± 0.8%).

Depolymerization of D11N/Q actins

I next used three different methods to analyze the depolymerization of D11N/Q polymers. In the first experiment, depolymerization was induced by addition of latrunculin A, which sequestered monomeric actin from the solution. After treatment for 10 min, the polymeric and depolymerized fractions were separated using ultracentrifugation and visualized using SDS-PAGE (Fig. 13A, B). After the latrunculin treatment, most of the WT actin was recovered in the supernatant fraction, whereas a majority of the D11N/Q actin was pelleted. Intriguingly, 1:1 WT-D11Q copolymers were also more resistant to latrunculin treatment than were WT homopolymers. In the second experiment, I copolymerized pyrenyl WT actin and D11Q actin; then following addition of latrunculin A, I monitored the reduction in pyrene fluorescence as an indicator of depolymerization of WT subunits within the copolymers (Fig. 13C). This experiment revealed that WT subunits copolymerized with D11Q actin were significantly slower to depolymerize than were WT homopolymer filaments.

The results summarized above suggest that not only are Asp11-mutant actins slow to depolymerize, they also slow the depolymerization of copolymerized WT actin. However, I was unable to rule

out the possibility that D11N/Q actins did not bind lactruculin A, or that the fluorescent signal observed in Figure 13B was derived from pyrenyl WT actin trapped within the rings or rod-like structures. Therefore, in the third experiment, copolymers of Alexa 488-labeled WT actin and unlabeled WT or D11Q actin were immobilized on glass surfaces coated with skeletal muscle heavy meromyosin; then after washing out the free monomeric actin, the depolymerization of individual filaments was followed by observation using fluorescence microscopy (Fig. 13D). Filaments often fragmented, presumably due to the strong excitation light, and very short fragments diffused away because the density of the heavy meromyosin molecules on the surface was low. I identified fragmentation events based on sequential images taken at 5-min intervals, and analyzed changes in the lengths of unfragmented filaments. WT homopolymer filaments shortened at a rate of 0.16 ± 0.083 μm/min (average ± SD, N=55), which is roughly consistent with the estimate for skeletal Mg-actin (0.1 μm/s) under slightly different buffer conditions (Fujiwara et al., 2002). By contrast, Alexa 488-WT/D11Q copolymer shortened at about half that rate (0.072 ± 0.049 μm/min; N=56). This finding qualitatively confirms the results of the latrunculin experiments and demonstrates that copolymerization with D11Q actin slows the depolymerization of WT actin within filaments.

Effect of Asp-11 Mutations on Nucleotide Exchange and Phosphate Release Rates

The strategic position of Asp-11 in the nucleotide binding pocket and the aberrant polymerization/ depolymerization properties of the Asp-11-mutant actins suggested that those mutant actins have altered nucleotide binding properties. Thus, I together with Dr. K. Ito of Chiba University first examined the release rates of bound nucleotides by measuring the decrease in the fluorescence of ε-ATP when bound ε-ATP was released in the presence of excess ATP (Fig. 14A). ε-ATP that was bound to WT actin was released at a rate of 0.012 ± 0.0029 s^{-1}, which is consistent with previous measurements using skeletal actin (Kudryashov et al., 2010; Miller and Trybus, 2008). In contrast, ε-ATP bound to monomeric D11Q actin was released at an ~40-fold faster rate of 0.42 ± 0.098 s^{-1}. Release from D11N actin was even 10-fold faster, at 4.0 ± 0.16 s^{-1}. I have not directly measured the affinities of WT or mutant actins for ATP, but the extremely rapid

dissociation of ε-ATP from the mutant actins suggested much lower affinity of monomeric mutant actins, especially of D11N actin, for ATP. This speculation and the fact that purified D11N actin loses competence to polymerize normal filaments (Fig. 10), as well as large batch-to batch variations among different D11N preparations (data not shown), suggested that D11N actin quickly denatured during and/or after dialysis against G-buffer containing 0.1 mM ATP. This precluded D11N actin from further quantitative biochemical characterizations, and Dr. Uyeda focused his subsequent analyses on D11Q actin.

I next compared the rates of nucleotide release from WT and D11Q filaments (Fig. 14B). Consistent with previous measurements that nucleotide release is very slow from skeletal actin filaments (Kitagawa et al., 1968; Martonosi et al., 1960; Strohman, 1959), the increase in fluorescence of ε-ATP was very small and slow, if at all, when phalloidin-stabilized WT filaments that were dialyzed against F-buffer containing 0.1mM ATP and then treated with the Dowex resin to remove free ATP were mixed with 0.1 mM ε-ATP. In contrast, a large increase in fluorescence intensity was observed with D11Q filaments over the 3-h time course. The time course did not fit a single exponential curve well, suggesting the presence of two or more different populations of D11Q subunits, such as the ATP-bound and ADP-bound forms or the normal filaments and oligomeric structures. In any case, it was clearly demonstrated that D11Q actin subunits in filaments release bound nucleotides much more rapidly than the WT subunits in filaments and rebind ATP.

A nearly stoichiometric amount of phosphate was released from polymerizing WT actin with a relatively short lag following an increase in light scattering (Fig. 10A). Phosphate was released from polymerizing D11Q actin as well, although the lag between polymerization and phosphate release was significantly larger with D11Q actin, suggesting either slower ATP hydrolysis or higher affinity for Pi after hydrolysis on D11Q actin subunits in filaments. Nonetheless, despite the rapid release of bound ATP, D11Q actin clearly retains the activity to hydrolyze ATP in a polymerization-dependent manner.

Effect of Asp11 mutation on cofilin binding and severing by cofilin

Cofilin is the major actin depolymerizing factor *in vivo* (Bernstein and Bamburg, 2010; Carlier, 1998), with activities to sever filaments (Maciver et al., 1991), depolymerize actin filaments (Mabuchi, 1981; Nishida et al., 1984), possibly by enhancing subunit dissociation from pointed ends of the filaments (Carlier et al., 1997), and bind to actin monomers (Mabuchi, 1981; Nishida et al., 1984). Thus, the effects of D11Q mutation on interactions with cofilin were next examined.

Cosedimentation of cofilin with actin polymers at pH 6.5, a condition under which cofilin binds to actin filaments without significantly depolymerizing them (Hawkins et al., 1993; Pavlov et al., 2006; Yonezawa et al., 1985), showed that, although WT filaments and copolymers of WT and D11Q actins bound cofilin with similar affinities, D11Q homopolymers hardly bound cofilin (Fig. 15A). However, it was not possible to determine unequivocally that D11Q subunits within normal homopolymer filaments bound cofilin, because unknown fractions of the mutant actin molecules were sequestered in oligomeric structures. Thus, mCherry-fused cofilin was added to Alexa-Fluor 488-labeled D11Q or WT filaments, and found under a fluorescence microscope that cofilin-mCherry hardly bound the D11Q filaments, although it bound and disassembled WT filaments (Fig. 15B).

Binding of cofilin to monomeric D11Q actin was next assayed by cross-linking in G-buffer. Although G-buffer has a very low concentration of salts and would enhance actin-cofilin binding more than under physiological conditions, monomeric D11Q actin was cross-linked to cofilin at a significantly slower rate than WT actin (Fig. 15C). Taken together, it was concluded that D11Q actin has lower affinities for cofilin in both filamentous and monomeric forms, as well as in the small oligomeric structures.

Next, the activities of cofilin against D11Q actin were assayed at pH8.3, the condition under which cofilin efficiently depolymerizes actin filaments (Hawkins et al., 1993; Pavlov et al., 2006; Yonezawa et al., 1985), using two different assays. In the first set of experiments, cofilin-induced depolymerization was assayed by ultracentrifugation followed by SDS-PAGE. Incubation with 10 μM cofilin for 15 min released more than half of the subunits to the supernatant fraction from the WT filaments. In contrast, copolymer filaments of Alexa-Fluor 488-WT actin and unlabeled D11Q actin were significantly resistant to depolymerization by cofilin (Fig. 16A).

Observation of gel fluorescence demonstrated that Alexa-Fluor-labeled WT actin was also protected from cofilin activity when copolymerized with D11Q actin (Fig. 16A). Densitometric scanning of the gels showed that cofilin-induced depolymerization of Alexa- Fluor 488-WT actin in copolymers with D11Q actin was 38 ± 9% (n = 3) of that in homopolymers.

In the second set of experiments, fluorescence microscopy was used to monitor the disappearance of WT homopolymer and WT/D11Q copolymer filaments. When 40 nM Alexa-Fluor 488-WT actin filaments were incubated with 2 μM cofilin, filaments disappeared almost completely within 6 min (Fig. 16B). In contrast, many filaments remained when 40 nM 1:1 copolymer filaments of Alexa-Fluor 488-WT and unlabeled D11Q actins were treated with 2 μM cofilin for 6 min. Some filaments remained even after 26 min (data not shown), further indicating that copolymer filaments of WT and D11Q actins were significantly resistant to the depolymerizing activity of cofilin.

Strikingly, when I performed cofilin-depolymerization assay in F-buffer that contained 1 mM ADP in addition to 0.1 mM ATP, cofilin was able to depolymerize D11Q filaments fairly efficiently, although not as efficiently as WT actin in the presence of ADP (Fig. 17). This result suggested that ADP in the buffer was incorporated into D11Q subunits in the filaments, due to the very rapid exchange of bound nucleotides, and made them susceptible to cofilin activity, whereas in the standard F-buffer that only contained ATP, most of the D11Q subunits carried bound ATP even if bound ATP was hydrolyzed to ADP, which conferred resistance to cofilin activity. Under a more physiological condition, *i.e.* in the presence of 1 mM ATP and 50 μM ADP (Williams et al., 1993), D11Q actin was resistant to cofilin activity, suggesting that D11Q actin subunits were resistant to cofilin activity *in vivo*.

Allosteric effect of Asp11 mutation on the structure of DNase loop

Finally, effects of Asp11 mutation on the structure of the DNase loop were examined. First, the structure of the DNase loop was monitored based on its susceptibility to cleavage by subtilisin (Muhlrad et al., 2004). SDS-PAGE analysis showed that in the presence of 1 μg/mL subtilisin, WT G-actin was cleaved almost completely within 5 min under our experimental

conditions. By contrast, D11Q G-actin was cleaved at a much slower rate under the same conditions (Fig.18A).

The DNase loop is involved in actin binding to DNase I and inhibiting the enzyme's activity (Kabsch et al., 1990; Lazarides and Lindberg, 1974). Again, D11Q actin bound to and inhibited DNase I much less efficiently than WT actin (Fig. 18B). Given that DNase I binds to monomeric actin, this finding, as well as the results of the subtilisin cleavage (Fig. 18A) and cofilin crosslinking (Fig. 15) experiments, suggest that the structure of the monomeric Asp11-mutant actin also significantly differs from the WT structure.

DISCUSSION

The Asp11 mutation has been shown to be dominantly negative both in yeast actin (Johannes and Gallwitz, 1991) and human α actin, the latter leading to congenital myopathy (Laing et al., 2009). *In vitro* characterizations reported here revealed that both D11N and D11Q mutant actins undergo salt-dependent reversible polymerization, and the resultant filaments appear normal when observed by low resolution electron microscopy. However, relatively few normal filaments were formed with purified D11N actin, presumably due to denaturation during overnight dialysis against G-buffer containing 0.1 mM ATP, which forced us to focus our detailed biochemical analyses on D11Q actin.

D11Q filaments move more or less normally on surfaces coated with skeletal heavy meromyosin (data not shown), and interaction of monomeric D11Q with profilin and thymosin β appeared normal as well in the context of fusion proteins *in vivo* (T. Uyeda, unpublished data). Nonetheless, D11Q actin showed a number of biochemical defects. For instance, D11Q actin filaments depolymerized more slowly than WT filaments, as did copolymer filaments of WT and D11Q actins (Fig. 13). Furthermore, both monomer and filament forms of D11Q rapidly exchanged bound nucleotides with free nucleotides in solution (Fig. 14), and failed to interact properly with cofilin (Figs. 15-18). ADP concentration is much lower than ATP in cells (Williams et al., 1993) as well as in standard G- and F-buffers, so that the rapid exchange of bound nucleotides would allow most of the D11Q actin molecules to carry ATP, even if the hydrolysis activity is normal, both *in vivo* and *in vitro*. ATP-bound skeletal actin is slower to depolymerize than ADP-bound actin (reviewed by (Korn et al., 1987)), and this may be at least one of the reasons why D11Q actin filaments are slower to depolymerize. In copolymer filaments of D11Q and WT, slow dissociation of ATP-bound D11Q subunits from depolymerizing ends would cause pauses, leading to slower average depolymerization rates of copolymers. Although my analyses on D11N actin were limited, I believe the same explanation is applicable to D11N actin since D11N actin monomers released bound nucleotides even more rapidly.

In cells, however, spontaneous depolymerization of actin filaments is unlikely to play any important roles, as the concentration of monomeric actin

is above the critical concentration for polymerization, and it is generally believed that cofilin-mediated depolymerization from the pointed ends of filaments is physiologically relevant (Carlier et al., 1997). D11Q actin monomers and homopolymers do not bind cofilin (Figs. 14 and 15), and render copolymer filaments with WT actin partially resistant to the depolymerizing activity of cofilin (Fig. 16). Considering very rapid turnover of actin subunits in dynamic structures within non-muscle cells (Murthy and Wadsworth, 2005; Theriot and Mitchison, 1991; Theriot et al., 1992), this slow depolymerization of copolymer filaments of WT and D11Q mutant actins may well be deleterious for non-muscle cells, including yeast. Again, the rapid exchange of bound nucleotides would explain why D11Q filaments do not bind cofilin, since the cellular concentration of ATP is much higher than that of ADP (Williams et al., 1993), and cofilin is unable to bind ATP-bound actin filaments (Carlier et al., 1997). This view is consistent with the fact that D11Q filaments were efficiently depolymerized by cofilin in F-buffer containing 1 mM ADP in place of ATP (Fig. 18).

The inability of monomeric D11Q actin molecules to bind cofilin would cause additional problems. The cellular concentration of total actin is well above the critical concentration for polymerization, and a number of actin-binding proteins are present to maintain a polymerization-competent monomeric actin pool. Although there is evidence against the simple idea that cofilin sequesters monomeric ADP-actin from polymerization (Blanchoin and Pollard, 1998), differential high affinity of cofilin for ADP-actin monomer over ATP-actin monomer (Carlier et al., 1997; Maciver and Weeds, 1994) suggests a role of cofilin in this complex process, which would not work with Asp11 mutant actins in the cells.

In light of the traditional notion that the turnover of sarcomeric actin is only slow in muscle cells (Zak et al., 1977), it is not intuitively obvious if the same cofilin-related explanations are applicable to the dominant negative effect of D11N mutation in the α actin gene leading to myopathy. However, it is now established that actin subunits turnover rapidly in both developing and mature muscle cells (reviewed by Ono, (2010)). Furthermore, cofilin is expressed in muscle cells (Nakashima et al., 2005), and recent studies provided evidence that mutation in cofilin causes nameline myopathy (Agrawal et al., 2007), and that cofilin is required for muscle development (Agrawal et al., 2012) and maintenance

(Miyauchi-Nomura et al., 2012). In the mutant muscle cells, D11N actin is probably present at the same concentration as WT. This would lead to a modest retardation of cofilin-mediated depolymerization of copolymer actin filaments and disturb the turnover of actin monomer, so that the mutant muscle cells become sick, but do not die. *Dictyostelium* cells expressing GFP-D11Q actin did not show noticeable defects in growth or cell morphology (data not shown). This is presumably because the relative content of GFP-D11Q actin was much less than that of endogenous actin, as was the case with other GFP-mutant actins (Noguchi et al., 2010b).

G146V is another dominant lethal actin mutation in yeast, which also inhibits cofilin binding (Noguchi et al., 2010a). The K336I mutation, which in human α actin causes congenital myopathy (Laing et al., 2009), also makes *Dictyostelium* actin incapable of binding cofilin (N. Umeki and T. Uyeda, unpublished data). Furthermore, the P332A mutation in γ actin, which causes autosomal dominant nonsyndromic progressive deafness, was resistant to depolymerization by cofilin (Bryan and Rubenstein, 2009). Taken together, I propose that a significant fraction of polymerization-competent dominant negative mutant actins exert toxic effects by dominantly disturbing cofilin-mediated dynamic regulation of the actin cytoskeleton. It was recently found that N12D mutation in the β actin gene causes Baraitser-Winter syndrome (Riviere et al., 2012), and it will be interesting to investigate if this mutation, which occurred right next to D11N in the opposite direction, increases or decreases the sensitivity to the cofilin activity.

A recent high resolution structural study demonstrated that the side chain of Asp11 indirectly interacts with the ß phosphate of ADP through a water molecule (Murakami et al., 2010). It thus makes sense that mutating Asp11 changes the affinity for nucleotides, although it is not intuitively obvious why changing to Asn causes a more severe phenotype than to Gln. I speculate that this modification of nucleotide binding affinity can explain much of the defective interaction of D11Q actin with cofilin. However, cofilin was unable to depolymerize D11Q actin filaments as efficiently as WT filaments even in the presence of 1 mM ADP. This may be due to slower ATP hydrolysis or Pi release from D11Q actin in filaments. Furthermore, the slower polymerization of Asp11 mutant actins is difficult to explain by rapid nucleotide exchange, together suggesting additional mechanisms by

which Asp11 mutations affect the interaction with cofilin and/or impair cellular function of the mutant actin. Mutation to Asp11 may allosterically affect the conformation of subdomain 2, as allosteric interactions between subdomain 2 and the nucleotide binding cleft (Combeau and Carlier, 1988; Muhlrad et al., 1994), including those involving cofilin (Muhlrad et al., 2006),have been reported. Thus, this allosteric effect of Asp11 mutations may impair the interaction with cofilin and other actin subunits during polymerization, since subdomain 2 of actin is a major binding site for cofilin (Galkin et al., 2001; McGough et al., 1997) as well as for the adjacent actin subunit on the pointed side within the same protofilament (Fujii et al., 2010; Holmes et al., 1990; Murakami et al., 2010; Oda et al., 2009). Detailed structural analyses of Asp11-mutant actins should shed light on these biologically important intramolecular communications.

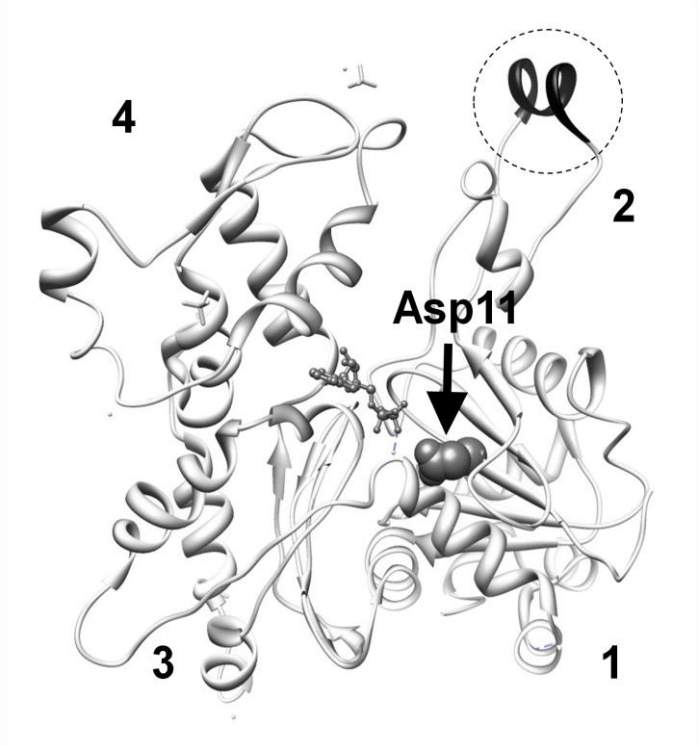

Figure 9. Conserved Asp11 shown in a space filling representation within the atomic structure of an actin filament (PDB ID: 3G37) (Murakami, et al., 2010). The DNase loop is modeled as a helix and is darkly colored at the upper right corner in this structure. Shown in a ball and stick representation is the bound ADP. Numbers show the subdomains.

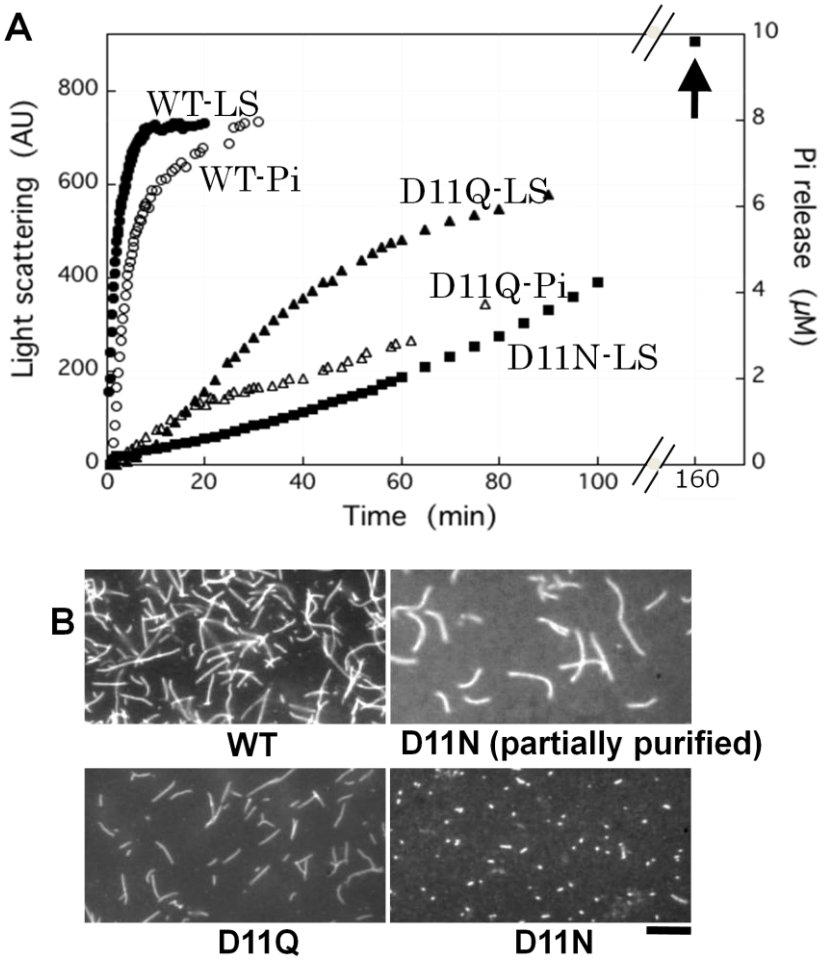

Figure 10. Polymerization of WT and Asp11 mutant actins. **A**: Polymerization of WT (filled circles), D11Q (*f*illed triangles), and D11N (filled squares) actin solutions. Final concentration of actin was 10 μM, and polymerization was monitored by the increase of light scattering at 360 nm (left abscissa). In parallel, release of phosphate from polymerizing WT (open circles) and D11Q (open triangles) actin was monitored using the EnzCheck phosphate assay kit (right abscissa). Arrow indicates light scattering of D11N actin polymer at 160 min. **B**: Fluorescence micrograph of WT, D11Q, and D11N actin filaments stained by rhodamine-phalloidin overnight at 5°C. For D11N actin, the partially purified fraction from Q-Sepharose column chromatography and the purified fraction by a depolymerization/polymerization cycle are shown. Bar: 10 μm. AU: arbitrary units.

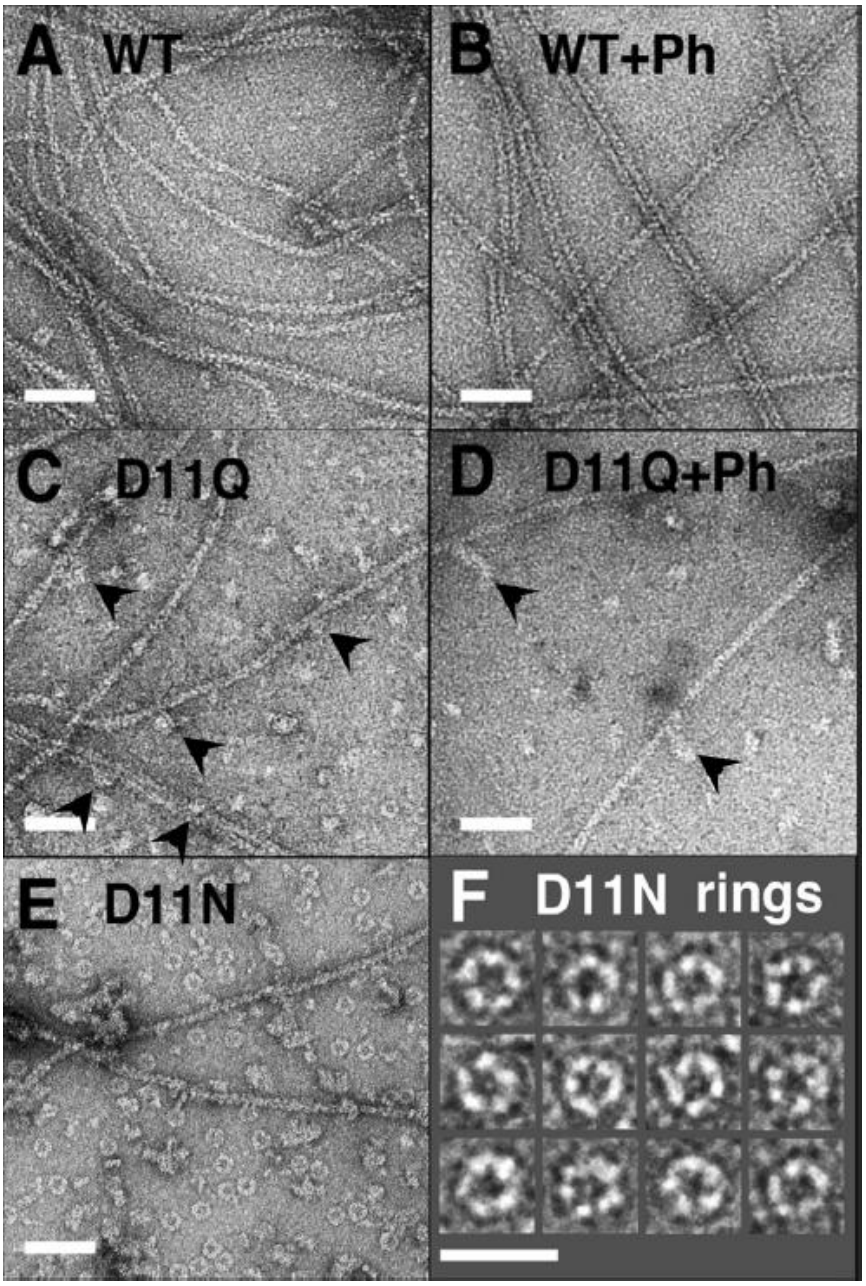

Figure 11. Electron micrographs of negatively stained actin polymers. WT (**A, B**), D11Q (**C, D**) and D11N (**E, F**) actins were polymerized in F-buffer in the absence (**A, C, E, F**) or presence (**B, D**) of 20 μM phalloidin for 2 h, diluted and stained with uranyl acetate. Arrowheads indicate oligomeric structures in D11Q polymers that are associated along the length of filaments. **F** is an enlarged image of the boxed area in (**E**). Bars are 50 nm, except for **F** (25 nm).

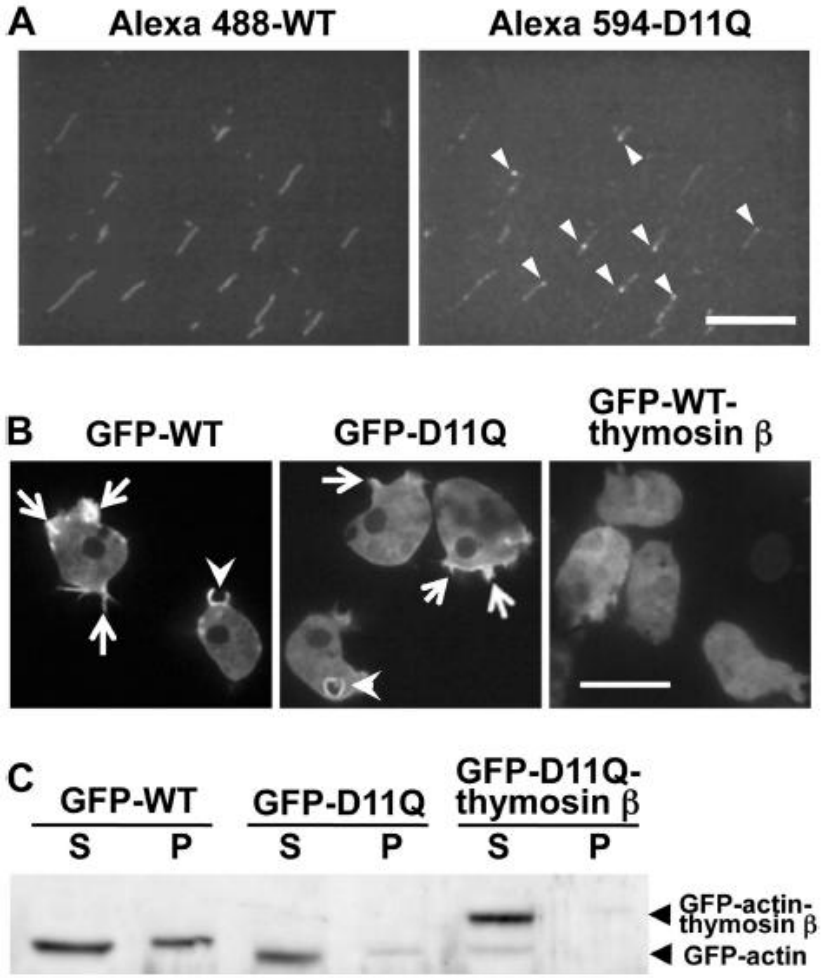

Figure 12. Copolymerization of WT and D11Q actin. **A**: Filaments obtainedby copolymerization of WTactin labeled with Alexa-Fluor 488 and D11Q actin labeled with Alexa-Fluor 594. The two fluorophores were observed in the green (left) and red fluorescence (right) channels, respectively. Arrowheads indicate puncta of Alexa-Fluor 594-D11Q actin within or along copolymers. Bar: 20 μm. **B**: Fluorescence micrograph of *Dictyostelium* cells expressing GFP-WT actin, GFP-D11Q actin, and GFP-WT actin fused with thymosin β. Arrows indicate the accumulation of GFP-actin along cell peripheries and thin projections, and arrowheads indicate enrichment around macropinocytic cups. Bar: 20 μm. **C** : Western blotting analysis of cells expressing GFP-WT actin, GFP-D11Q actin, or GFP-D11Q actin fused with thymosin β. Triton-soluble (S) and -insoluble (P) fractions were separated by SDS-PAGE and probed with anti-GFP antibodies.

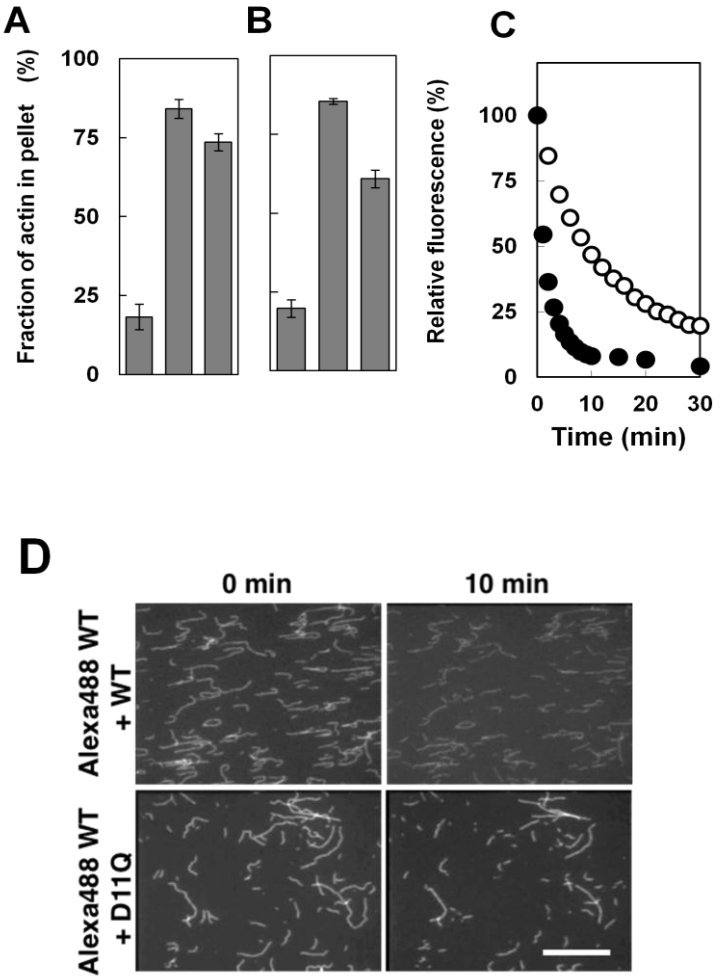

Figure 13. Depolymerization of D11N/Q actins. **A, B**: Latrunculin-induced depolymerization of D11Q and D11N actins. Solutions of polymers of WT or mutant actin or a 1:1 mixture of the two were ultracentrifuged with or without preincubation for 10 min with 60 μM latrunculin A. The supernatant and pellet fractions were analyzed by SDS-PAGE, and the fractions in pellets were determined using densitometry. Error bars indicate the standard deviation of three independent measurements. **C**: Latrunculin-induced depolymerization of pyrenyl WT actin copolymerized with the same concentration of unlabeled WT (filled circles) or D11Q (open circles) actin and assayed as in **A**. **D**: Depolymerization of individual actin filaments. Alexa 488-labeled WT actin copolymerized with the same concentration of unlabeled WT or D11Q actin was immobilized on heavy meromyosin-coated surfaces and imaged immediately and 10 min after flushing with buffer without actin. Bar: 20 μm.

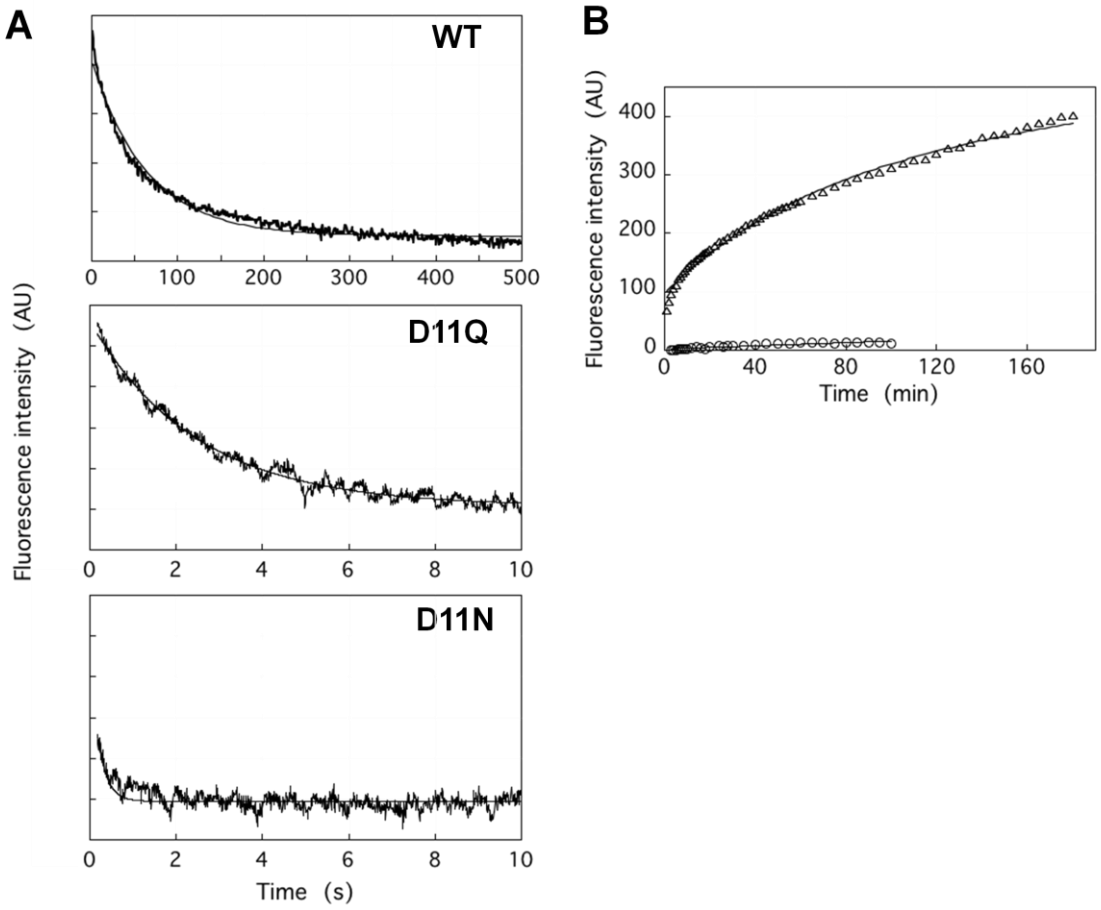

Figure 14. Nucleotide release from WT and Asp11 mutant actins. **A**: Release of ε-ATP from monomeric actin was assayed using a stopped flow apparatus. An actin solution dialyzed against G-buffer containing 0.2 mM ε-ATP was rapidly mixed with an equal volume of G-buffer containing 1 mM Ca-ATP. The averages of 3, 7 and 7 traces of WT, D11Q and D11N actins, respectively are shown, and the fine solid line shows fitting with single-exponentials. **B**: Exchange of filament-bound ATP with exogenous ε-ATP, as assayed by an increase in fluorescence following the addition of 0.1 mM ε-ATP to solutions of WT (circles) or D11Q (triangles) actin filaments dialyzed against F-buffer containing 0.1 mM ATP and then treated with Dowex resin to remove free ATP. Solid lines show fitting with single (WT) and double (D11Q) exponentials.

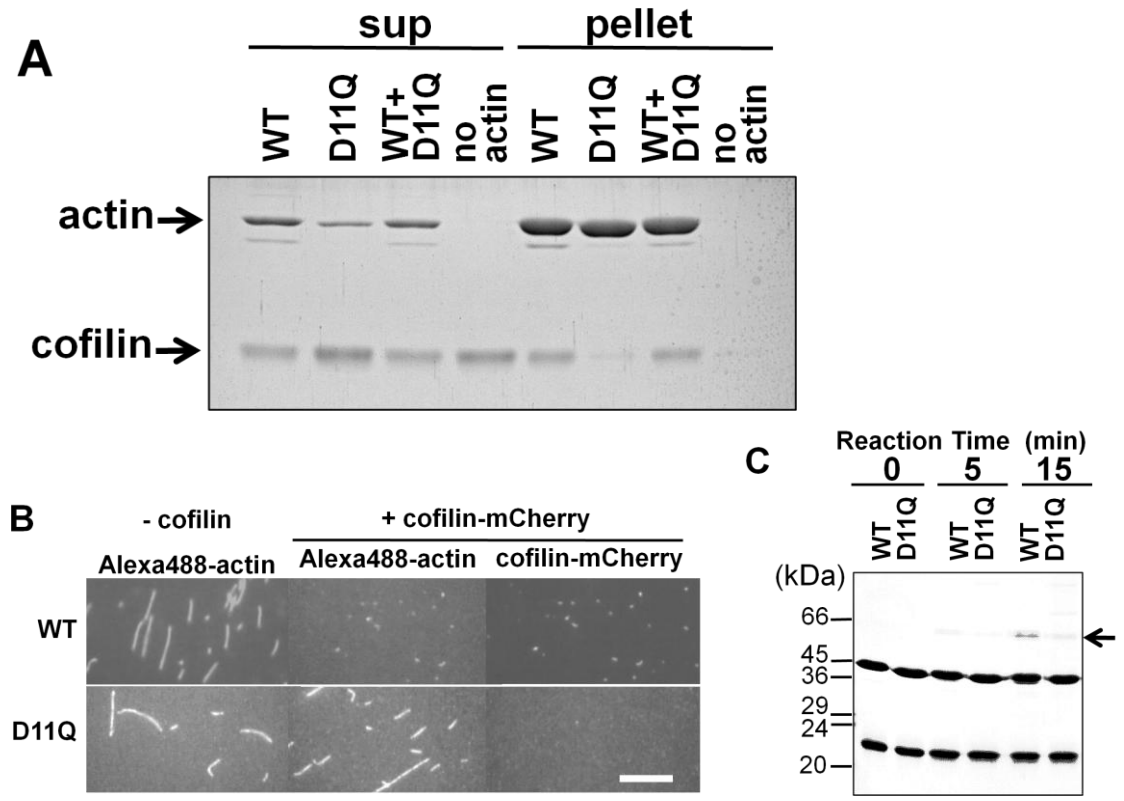

Figure 15. Cofilin binding. **A**: Cosedimentation of 5 μM WT, D11Q and 1:1 mixture polymers with 2.5 μM cofilin at pH 6.5. Supernatant and pellet fractions after ultracentrifugation were analyzed by SDS-PAGE. Densitometric analyses of three sets of data showed that 49.5 ± 4.7%, 0.57 ± 0.09% and 42.8 ± 2.1% of cofilin cosedimented with WT, D11Q and WT+D11Q filaments, respectively. **B**: Fluorescence microscopic observation of binding of cofilin-mCherry to WT or D11Q actin filaments labeled with Alexa Fluor 488. Bar: 15 μm. **C**: Cofilin binding to monomeric actin. Binding of 14 μM cofilin to 7 μM monomeric WT or D11Q actin in G-buffer, detected by crosslinking with 40 mM EDC for 5 min, followed by SDS-PAGE. Arrow shows the position of the crosslinked actin-cofilin. Average of three independent measurements indicated that the crosslinking of D11Q actin was 47% ± 15% slower than WT actin, and this difference is statistically significant with $p<0.16$ by *Student*'s *t*-test. Higher molecular weight ladders formed in D11Q-cofilin cross-link reactions were formed even when D11N or D11Q actin, but not WT actin, was treated with 1-ethyl-3-(3-dimethylaminopropyl) carbodiimide in G-buffer in the absence of cofilin.

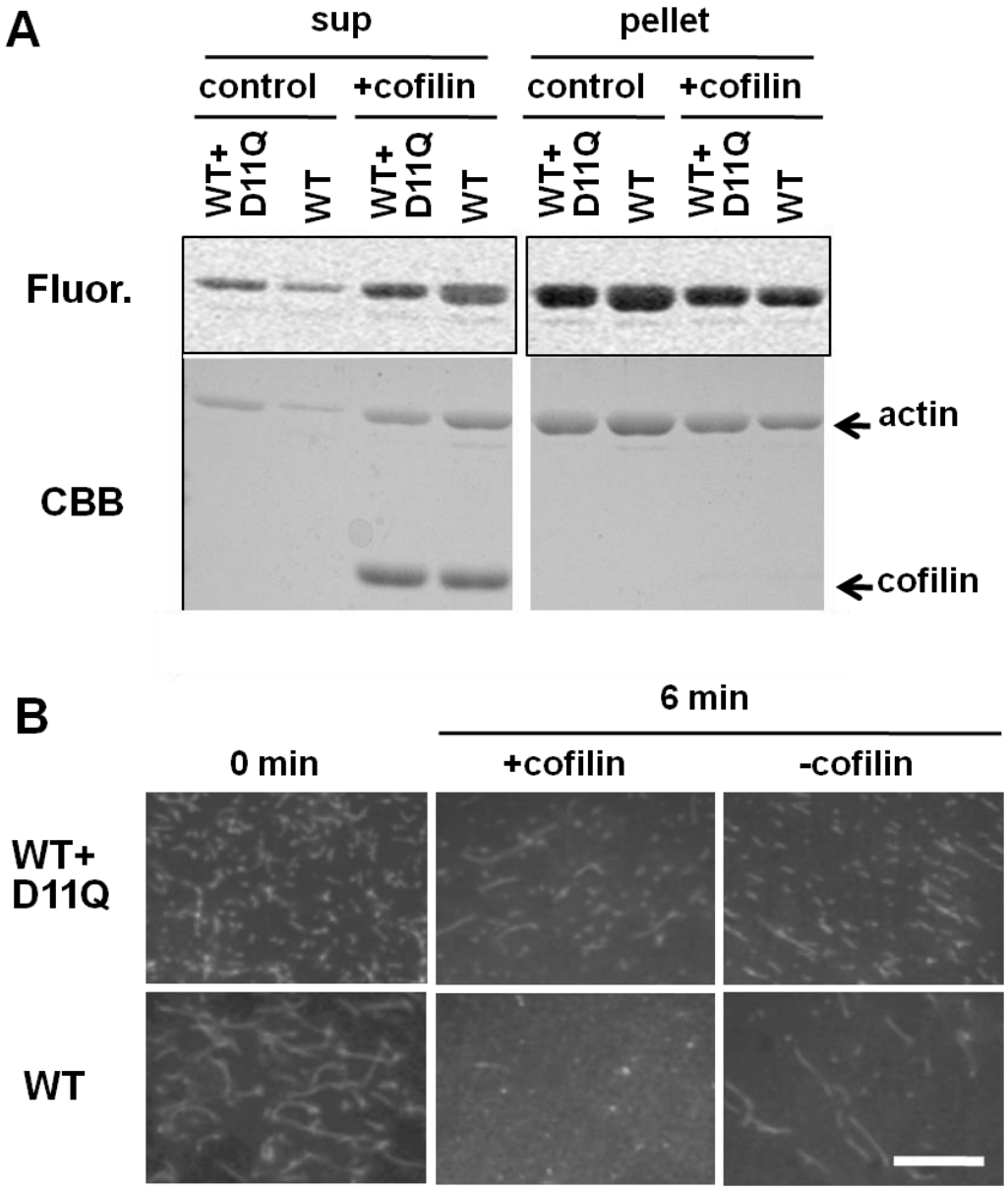

Figure 16. Cofilin-induced depolymerization. **A**: 5 μM WT actin filaments and a 1:1 mixture of WT and D11Q actin polymers were treated with 10 μM cofilin at pH 8.3, and after incubation for 15 min, the mixtures were subjected to ultracentrifugation followed by SDS-PAGE of the supernatant and pellet fractions. 2.5 μM WT actin was labeled with Alexa Fluor 488. Fluorogram visualized WT subunits only and Coomassie stained both WT and mutant actins. **B**: Fluorescence microscopic observation of cofilin-induced depolymerization of Alexa Fluor 488-labaled WT filaments and 1:1 copolymer of labeled WT and unlabeled D11Q actin. Bar: 20 μm

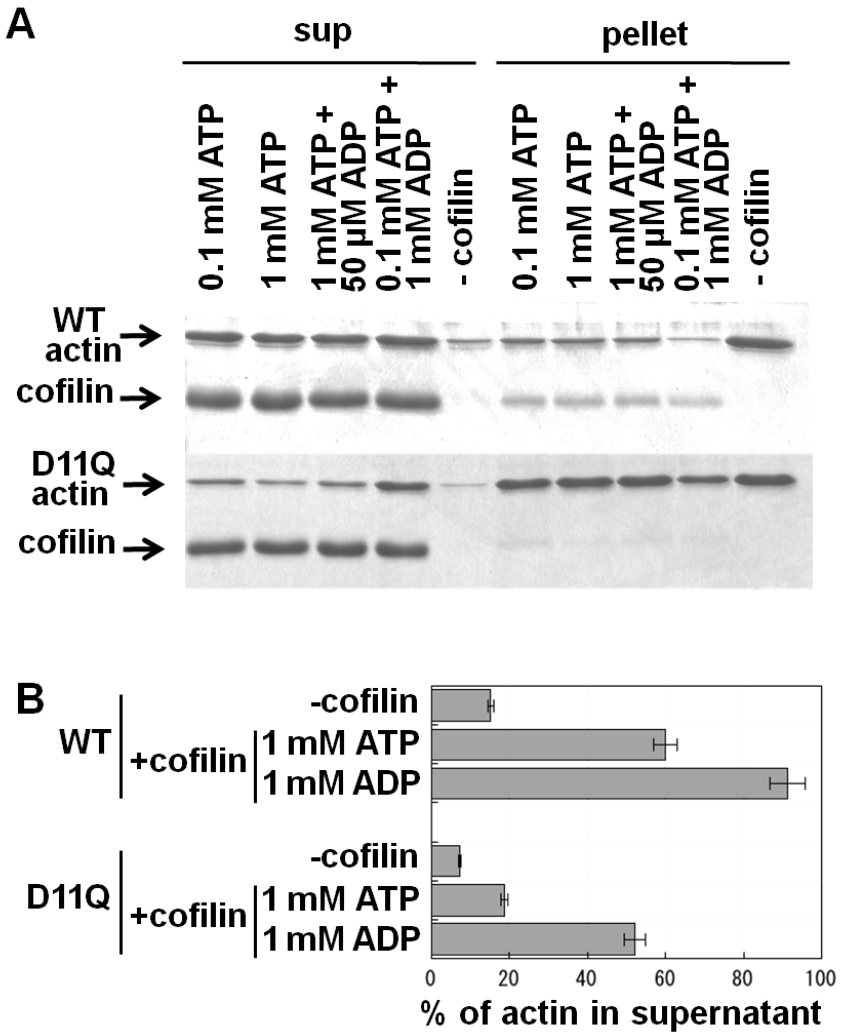

Figure 17. Effects of ADP on cofilin-mediated depolymerization of actin filaments. WT or D11Q actin filaments in F-buffer containing 0.1 mM ATP were diluted to 5 µM in F-buffer that contained 2 mM Hepes pH 7.4 and various concentrations of nucleotides. After 30 min of incubation, concentrated Hepes buffer pH 8.35 and cofilin were added to a final concentration of 10 mM and 10 µM, respectively. After incubation for 15 min, the mixtures were subjected to ultracentrifugation and supernatant and pellet fractions were analyzed by SDS-PAGE. **A** is a representative of three independent sets experiments. **B** shows the average and standard deviation of the three sets of data. The difference between cofilin-induced depolymerizatio of WT actin and D11Q actin in the presence of 1 mM ATP, as well as that of D11Q actin between 1 mM ATP and 1 mM ADP, were statistically significant by Student's *t*-test ($p<0.001$).

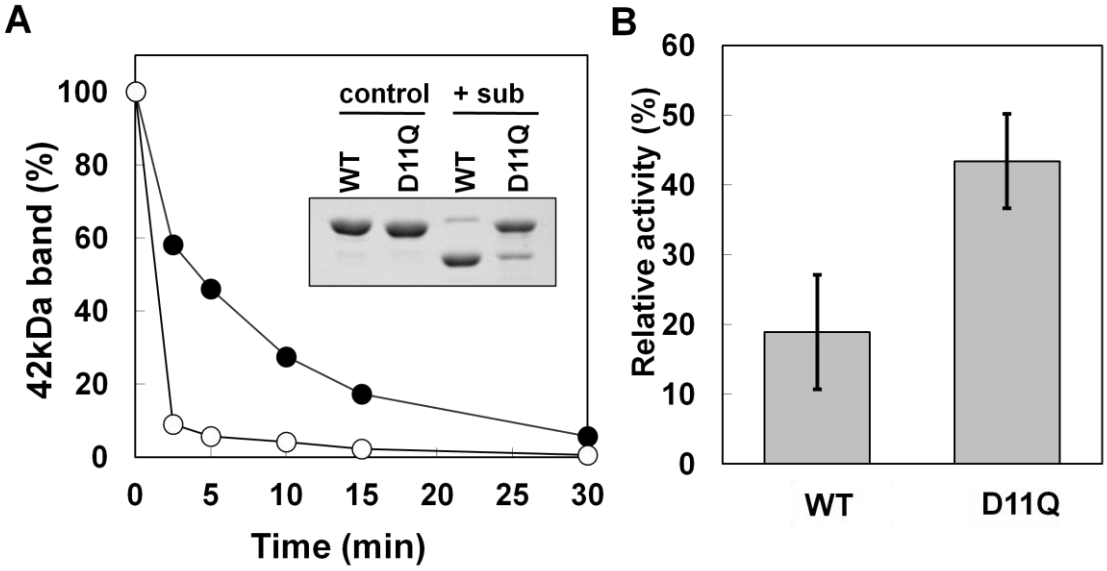

Figure 18. Effects of D11Q mutation on the conformation of the DNase loop in monomeric actin. Time course of the subtilisin cleavage of monomeric WT and D11Q actins in G-buffer, as assayed by SDS-PAGE and densitometry of the stained gel. Inset: SDS-PAGE of WT and D11Q actins at 0 (control) and 2.5 min (+sub) of incubation with 1 μg/mL subtilisin. **B**: Inhibitory effect of WT and D11Q actins on the activity of DNase I. Student's *t*-test on three independent sets of data indicated that the difference is significant with p=0.016.

General Discussion

Interactions between actin and cofilin play critical roles in regulating the cytoskeletal reorganizations, and this study was carried out to understand the molecular mechanisms behind those processes, with a special emphasis on the differences in actin-bound nucleotides.

In Chapter I entitled "Effects of bound nucleotide on the affinity of actin for cofilin", I was able to observe cooperative binding of human cofilin to actin filaments using fluorescence microscopy. Cooperative binding of cofilin to actin filaments, and cooperative conformational changes of actin filaments that accompany the cooperative binding, have been observed using electron microscopy (Galkin et al., 2001; McGough et al., 1997). If the cooperative structural changes of actin filaments play roles in the cooperative binding of cofilin to actin filaments in the cells, it would be necessary to observe cooperative binding of cofilin to actin filaments with an observation field of the scale of cells, i.e., in the range of micrometers. Fields of view of electron microscopes are too narrow for this purpose, and the present study, which used fluorescence microscopy, demonstrated that cooperative binding occurs in the length scale of micrometers along actin filaments. Suarez et al. independently reached the same conclusion (Suarez et al., 2011).

Theoretically, cooperative binding of cofilin to actin filaments could occur through two different mechanisms. In one model, affinity between cofilin molecules could drive formation of clusters, i.e., cooperative binding, along actin filaments. However, recent high resolution electron microscopic structural analysis showed that cofilin molecules in clusters along actin filaments do not directly contact the neighbor molecules (Galkin et al., 2011), ruling out this possibility. The second model assumes that cofilin binding induces a specific conformational change in bound actin subunits, and this conformational change is propagated to neighbor actin subunits, which in turn increases the affinity of that neighbor subunit for a new cofilin molecule. Because binding of cofilin causes major structural changes in bound actin subunits, including supertwisting of the helix by 25% (Galkin et al., 2001; McGough et al., 1997), it is reasonable to speculate that the supertwisted conformation of actin filaments in cofilin clusters is propagated to neighbor actin subunits and attracts more cofilin binding. Until very recently, this second model has been hypothetical, but Ngo, Kodera and their colleagues

recently demonstrated by high speed atomic force microscopy that the supertwisted conformation is actually propagated to neighbor actin subunits, and more cofilin molecules bind to the newly supertwisted segment of the filament (Ngo et al., manuscript in preparation). Other actin-binding proteins, including the motor domain of myosin II (Orlova and Egelman, 1997; Tokuraku et al., 2009), drebrin (Sharma et al., 2012), α-catenin (Hansen et al., 2013), fimbrin (Volkmann et al., 2001), and tropomyosin (Butters et al., 1993) have been shown to bind actin filaments cooperatively, and those cooperative bindings may also depend on cooperative structural changes of actin filaments. In particular, binding of myosin II motor domain was shown to change the structure of actin filaments, including untwisting of the helical pitch (Tsaturyan et al., 2005). It is notable that this untwisting conformational change of actin filaments induced by myosin II is completely different from the supertwisting structural changes induced by cofilin. Thus, Uyeda et al. (2011) speculated that cofilin cannot bind to actin filaments to which myosin II is already bound cooperatively, and conversely, myosin II cannot bind to actin filaments to which cofilin is already bound cooperatively. This hypothesis can be generalized that cooperative conformational changes of an actin filament play important roles in selecting the actin-binding protein, and hence, specifying the function of the actin filament (Galkin et al., 2012; Michelot and Drubin, 2011; Romet-Lemonne and Jegou, 2013; Schoenenberger et al., 2011; Tokuraku et al., 2009; Uyeda et al., 2011). I anticipate that the results of the present study, which demonstrated cooperative binding of cofilin in the micrometer range, would provide useful framework to elucidate the control mechanism of the actin cytoskeleton.

In addition, I demonstrated that human cofilin efficiently binds actin filaments carrying ADP in a cooperative manner, but almost not at all to those carrying ADP and Pi. This result is consistent with the aforementioned fluorescence microscopic analyses of yeast cofilin (Suarez et al., 2011) as well as classic biochemical analyses (Blanchoin and Pollard, 1999; Carlier et al., 1997). As I have discussed in Chapter I, actin monomers in the cells carry bound ATP. When incorporated into a filament from the barbed-end, hydrolysis of ATP is stimulated (Murakami et al., 2010) and eventually Pi is released. Thus, actin subunit with bound ATP is restricted to the barbed-end of the filament, while the ADP-bound form

accumulates near the pointed end (reviewed by Carlier, (1990)). Consequently, the property of cofilin to bind cooperatively to actin subunits carrying ADP would bias cofilin binding to, and severing of, the older parts of the actin filaments, and this may be physiological important for proper reconstruction of the actin cytoskeleton.

In Chapter II entitled "Characterization of Dominant Negative Asp11 Mutant Actins", with the help of colleagues in the laboratory, I analyzed biochemical properties of the D11Q mutant actin that was shown by a previous yeast study to be dominant lethal (Johannes and Gallwitz, 1991), and a similar D11N mutation in α-actin that causes congenital myopathy in human (Laing et al., 2009). I showed that, these mutant actins exchange bound nucleotides very quickly, even when in filaments, with that in external solution. In cells, ATP concentration is much higher than that of ADP, and therefore, this property of the Asp11 mutant actins would render the majority of molecules ATP-bound. Because cofilin binds preferentially to actin subunits carrying ADP as described above, these Aps11 mutant actins become resistant to the binding of and severing by cofilin. Interestingly, co-filaments of wild-type and D11Q mutant actins were also less susceptible to the severing action of cofilin. This is probably related to the requirement of cooperative conformational changes of actin filaments for cofilin binding, assuming that the Asp11 mutant actin molecules in co-polymers interfere with the cooperative conformational changes. This last property of the Asp11 mutant actins is presumably the reason why the mutant actins are not only non-functional but also dominantly toxic, in a sense that the protein is harmful to the cells even in the presence of wild type molecules. In conclusion, this study demonstrated the critical importance of very slow nucleotide exchange at actin subunits within filaments.

It will be interesting in the future to unveil the detailed molecular mechanism of cofilin-induced cooperative structural changes in actin filaments. Copolymers of wild type and D11Q mutant actin may be useful material in those studies. Improvements in the methods of fluorescence microscopic observation for live imaging of cofilin-actin interactions would also lead to useful kinetic and mechanistic insights.

Acknowledgements

I have had great fortune to have interacted with a number of talented people during my time in the Uyeda group.

First and foremost, I wish to thank my advisor, Professor Taro Q. P Uyeda, for giving me the opportunity to be here, guidance, advice and support. I could not have achieved this research without his support.

I wish thank Dr. Nobuhisa Umeki for his help in assays on Asp11 mutant actins. I could not have achieved this research without his cooperation.

I wish to thank Dr. Keiko Hirose for her help in electron microscopy. I also thank Dr. Kohji Ito for performing nucleotide exchange assay.

I also thank Dr. Taro Q. P. Noguchi, Dr. Kiyotaka Tokuraku and Dr. Akira Nagasaki. They gave me many advices for this research.

Most importantly, I thank my family for support and encouragement. None of this could have been achieved without them.

References

Agrawal, P.B., R.S. Greenleaf, K.K. Tomczak, V.L. Lehtokari, C. Wallgren-Pettersson, W. Wallefeld, N.G. Laing, B.T. Darras, S.K. Maciver, P.R. Dormitzer, and A.H. Beggs. 2007. Nemaline myopathy with minicores caused by mutation of the CFL2 gene encoding the skeletal muscle actin-binding protein, cofilin-2. *Am. J. Hum. Genet.* 80:162-167.

Agrawal, P.B., M. Joshi, T. Savic, Z. Chen, and A.H. Beggs. 2012. Normal myofibrillar development followed by progressive sarcomeric disruption with actin accumulations in a mouse Cfl2 knockout demonstrates requirement of cofilin-2 for muscle maintenance. *Hum Mol Genet*. 21:2341-2356.

Aizawa, H., Y. Fukui, and I. Yahara. 1997. Live dynamics of Dictyostelium cofilin suggests a role in remodeling actin latticework into bundles. *J Cell Sci*. 110 (Pt 19):2333-2344.

Aizawa, H., K. Sutoh, S. Tsubuki, S. Kawashima, A. Ishii, and I. Yahara. 1995. Identification, characterization, and intracellular distribution of cofilin in Dictyostelium discoideum. *J Biol Chem*. 270:10923-10932.

An, H.S., and K. Mogami. 1996. Isolation of 88F actin mutants of *Drosophila melanogaster* and possible alterations in the mutant actin structures. *J. Mol. Biol.* 260:492-505.

Bernstein, B.W., and J.R. Bamburg. 2010. ADF/cofilin: a functional node in cell biology. *Trends Cell Biol.* 20:187-195.

Blanchoin, L., and T.D. Pollard. 1998. Interaction of actin monomers with *Acanthamoeba* actophorin (ADF/cofilin) and profilin. *J. Biol. Chem.* 273:25106-25111.

Blanchoin, L., and T.D. Pollard. 1999. Mechanism of interaction of Acanthamoeba actophorin (ADF/Cofilin) with actin filaments. *J Biol Chem*. 274:15538-15546.

Bonder, E.M., D.J. Fishkind, and M.S. Mooseker. 1983. Direct measurement of critical concentrations and assembly rate constants at the two ends of an actin filament. *Cell*. 34:491-501.

Bryan, K.E., and P.A. Rubenstein. 2009. Allele-specific effects of human deafness gamma-actin mutations (DFNA20/26) on the actin/cofilin interaction. *J. Biol. Chem.* 284:18260-18269.

Burt, C.T., T. Glonek, and M. Barany. 1977. Analysis of living tissue by phosphorus-31 magnetic resonance. *Science*. 195:145-149.

Butters, C.A., K.A. Willadsen, and L.S. Tobacman. 1993. Cooperative interactions between adjacent troponin-tropomyosin complexes may be transmitted through the actin filament. *J Biol Chem*. 268:15565-15570.

Carlier, M.F. 1990. Actin polymerization and ATP hydrolysis. *Adv Biophys*. 26:51-73.

Carlier, M.F. 1998. Control of actin dynamics. *Curr. Opin. Cell Biol.* 10:45-51.

Carlier, M.F., V. Laurent, J. Santolini, R. Melki, D. Didry, G.X. Xia, Y. Hong, N.H. Chua, and D. Pantaloni. 1997. Actin depolymerizing factor (ADF/cofilin) enhances the rate of filament turnover: implication in actin-based motility. *J. Cell Biol.* 136:1307-1322.

Carlier, M.F., and D. Pantaloni. 1988. Binding of phosphate to F-ADP-actin and role of F-ADP-Pi-actin in ATP-actin polymerization. *J Biol Chem*. 263:817-825.

Combeau, C., and M.F. Carlier. 1988. Probing the mechanism of ATP hydrolysis on F-actin using vanadate and the structural analogs of phosphate BeF-3 and A1F-4. *J. Biol. Chem.* 263:17429-17436.

Cooke, R. 1975. The role of the bound nucleotide in the polymerization of actin. *Biochemistry*. 14:3250-3256.

De La Cruz, E.M. 2009. How cofilin severs an actin filament. *Biophys Rev*. 1:51-59.

Drummond, D.R., E.S. Hennessey, and J.C. Sparrow. 1991. Characterisation of missense mutations in the Act88F gene of *Drosophila melanogaster*. *Mol. Gen. Genet.* 226:70-80.

Egelhoff, T.T., M.A. Titus, D.J. Manstein, K.M. Ruppel, and J.A. Spudich. 1991. Molecular genetic tools for study of the cytoskeleton in Dictyostelium. *Methods Enzymol.* 196:319-334.

Fujii, T., A.H. Iwane, T. Yanagida, and K. Namba. 2010. Direct visualization of secondary structures of F-actin by electron cryomicroscopy. *Nature*. 467:724-728.

Fujiwara, I., S. Takahashi, H. Tadakuma, T. Funatsu, and S. Ishiwata. 2002. Microscopic analysis of polymerization dynamics with individual actin filaments. *Nat. Cell Biol.* 4:666-673.

Fujiwara, I., D. Vavylonis, and T.D. Pollard. 2007. Polymerization kinetics of

ADP- and ADP-Pi-actin determined by fluorescence microscopy. *Proc Natl Acad Sci U S A*. 104:8827-8832.

Galkin, V.E., A. Orlova, and E.H. Egelman. 2012. Actin filaments as tension sensors. *Curr Biol*. 22:R96-101.

Galkin, V.E., A. Orlova, D.S. Kudryashov, A. Solodukhin, E. Reisler, G.F. Schroder, and E.H. Egelman. 2011. Remodeling of actin filaments by ADF/cofilin proteins. *Proc. Natl. Acad. Sci. U. S. A.* 108:20568-20572.

Galkin, V.E., A. Orlova, N. Lukoyanova, W. Wriggers, and E.H. Egelman. 2001. Actin depolymerizing factor stabilizes an existing state of F-actin and can change the tilt of F-actin subunits. *J. Cell Biol.* 153:75-86.

Glotzer, M. 2001. Animal cell cytokinesis. *Annu Rev Cell Dev Biol*. 17:351-86.

Goode, B.L., D.G. Drubin, and G. Barnes. 2000. Functional cooperation between the microtubule and actin cytoskeletons. *Curr Opin Cell Biol*. 12:63-71.

Graceffa, P., and Dominguez, R. 2003. Crystal structure of monomeric actin in the ATP state. Structural basis of nucleotide-dependent actin dynamics. *J.Biol.Chem.* 278:34172-34180.

Hansen, S.D., A.V. Kwiatkowski, C.Y. Ouyang, H. Liu, S. Pokutta, S.C. Watkins, N. Volkmann, D. Hanein, W.I. Weis, R.D. Mullins, and W.J. Nelson. 2013. aE-catenin actin-binding domain alters actin filament conformation and regulates binding of nucleation and disassembly factors. *Mol Biol Cell*. 24:3710-3720.

Hatano, S., and F. Oosawa. 1966. Extraction of an actin-like protein from the plasmodium of a myxomycete and its interaction with myosin A from rabbit striated muscle. *J Cell Physiol*. 68:197-202.

Hawkins, M., B. Pope, S.K. Maciver, and A.G. Weeds. 1993. Human actin depolymerizing factor mediates a pH-sensitive destruction of actin filaments. *Biochemistry*. 32:9985-9993.

Hayden, S.M., P.S. Miller, A. Brauweiler, and J.R. Bamburg. 1993. Analysis of the interactions of actin depolymerizing factor with G- and F-actin. *Biochemistry*. 32:9994-10004.

Hendzel, M.J. 2014. The F-act's of nuclear actin. *Curr Opin Cell Biol*. 28C:84-89.

Holmes, K.C., D. Popp, W. Gebhard, and W. Kabsch. 1990. Atomic model of the actin filament. *Nature*. 347:44-49.

Hotulainen, P., E. Paunola, M.K. Vartiainen, and P. Lappalainen. 2005. Actin-depolymerizing factor and cofilin-1 play overlapping roles in promoting rapid F-actin depolymerization in mammalian nonmuscle cells. *Mol Biol Cell*. 16:649-664.

Iida, K., K. Moriyama, S. Matsumoto, H. Kawasaki, E. Nishida, and I. Yahara. 1993. Isolation of a yeast essential gene, COF1, that encodes a homologue of mammalian cofilin, a low-M(r) actin-binding and depolymerizing protein. *Gene*. 124:115-120.

Johannes, F.J., and D. Gallwitz. 1991. Site-directed mutagenesis of the yeast actin gene: a test for actin function in vivo. *EMBO J.* 10:3951-3958.

Kabsch, W., H.G. Mannherz, D. Suck, E.F. Pai, and K.C. Holmes. 1990. Atomic structure of the actin:DNase I complex. *Nature*. 347:37-44.

Kasai, M., S. Asakura, and F. Oosawa. 1962. The G-F equilibrium in actin solutions under various conditions. *Biochim Biophys Acta*. 57:13-21.

Kitagawa, S., W. Drabikowski, and J. Gergely. 1968. Exchange and release of the bound nucleotide of F-actin. *Arch. Biochem. Biophys.* 125:706-714.

Kondo, H., and S. Ishiwata. 1976. Uni-directional growth of F-actin. *J Biochem*. 79:159-171.

Korn, E.D., M.F. Carlier, and D. Pantaloni. 1987. Actin polymerization and ATP hydrolysis. *Science*. 238:638-644.

Kouyama, T., and K. Mihashi. 1981. Fluorimetry study of *N*-(1-pyrenyl)iodoacetamide-labelled F-actin. Local structural change of actin protomer both on polymerization and on binding of heavy meromyosin. *Eur. J. Biochem.* 114:33-38.

Kudryashov, D.S., E.E. Grintsevich, P.A. Rubenstein, and E. Reisler. 2010. A nucleotide state-sensing region on actin. *J. Biol. Chem.* 285:25591-25601.

Laing, N.G., D.E. Dye, C. Wallgren-Pettersson, G. Richard, N. Monnier, S. Lillis, T.L. Winder, H. Lochmuller, C. Graziano, S. Mitrani-Rosenbaum, D. Twomey, J.C. Sparrow, A.H. Beggs, and K.J. Nowak. 2009. Mutations and polymorphisms of the skeletal muscle alpha-actin gene (ACTA1). *Hum. Mutat.* 30:1267-1277.

Lappalainen, P., and D.G. Drubin. 1997. Cofilin promotes rapid actin filament turnover in vivo. *Nature*. 388:78-82.

Lazarides, E., and U. Lindberg. 1974. Actin is the naturally occurring inhibitor of deoxyribonuclease I. *Proc. Natl. Acad. Sci. U. S. A.*

71:4742-4746.

Mabuchi, I. 1981. Purification from starfish eggs of a protein that depolymerizes actin. *J. Biochem.* 89:1341-1344.

Maciver, S.K., and A.G. Weeds. 1994. Actophorin preferentially binds monomeric ADP-actin over ATP-bound actin: consequences for cell locomotion. *FEBS Lett.* 347:251-256.

Maciver, S.K., H.G. Zot, and T.D. Pollard. 1991. Characterization of actin filament severing by actophorin from Acanthamoeba castellanii. *J. Cell Biol.* 115:1611-1620.

Martonosi, A., M.A. Gouvea, and J. Gergerly. 1960. Studies on actin. I. The interaction of C14-labeled adenine nucleotides with actin. *J Biol Chem.* 235:1700-1703.

McGough, A., B. Pope, W. Chiu, and A. Weeds. 1997. Cofilin changes the twist of F-actin: implications for actin filament dynamics and cellular function. *J. Cell Biol.* 138:771-781.

Michelot, A., and D.G. Drubin. 2011. Building distinct actin filament networks in a common cytoplasm. *Curr Biol.* 21:R560-569.

Miller, B.M., and K.M. Trybus. 2008. Functional effects of nemaline myopathy mutations on human skeletal alpha-actin. *J. Biol. Chem.* 283:19379-19388.

Mitchison, T.J., and L.P. Cramer. 1996. Actin-based cell motility and cell locomotion. *Cell.* 84:371-379.

Miyauchi-Nomura, S., T. Obinata, and N. Sato. 2012. Cofilin is required for organization of sarcomeric actin filaments in chicken skeletal muscle cells. *Cytoskeleton (Hoboken).* 69:290-302.

Monserrat, L., M. Hermida-Prieto, X. Fernandez, I. Rodriguez, C. Dumont, L. Cazon, M.G. Cuesta, C. Gonzalez-Juanatey, J. Peteiro, N. Alvarez, M. Penas-Lado, and A. Castro-Beiras. 2007. Mutation in the alpha-cardiac actin gene associated with apical hypertrophic cardiomyopathy, left ventricular non-compaction, and septal defects. *Eur. Heart J.* 28:1953-1961.

Moon, A.L., P.A. Janmey, K.A. Louie, and D.G. Drubin. 1993. Cofilin is an essential component of the yeast cortical cytoskeleton. *J Cell Biol.* 120:421-435.

Morita, H., H.L. Rehm, A. Menesses, B. McDonough, A.E. Roberts, R. Kucherlapati, J.A. Towbin, J.G. Seidman, and C.E. Seidman. 2008.

Shared genetic causes of cardiac hypertrophy in children and adults. *N. Engl. J. Med.* 358:1899-1908.

Muhlrad, A., P. Cheung, B.C. Phan, C. Miller, and E. Reisler. 1994. Dynamic properties of actin. Structural changes induced by beryllium fluoride. *J. Biol. Chem.* 269:11852-11858.

Muhlrad, A., D. Kudryashov, Y. Michael Peyser, A.A. Bobkov, S.C. Almo, and E. Reisler. 2004. Cofilin induced conformational changes in F-actin expose subdomain 2 to proteolysis. *J. Mol. Biol.* 342:1559-1567.

Muhlrad, A., I. Ringel, D. Pavlov, Y.M. Peyser, and E. Reisler. 2006. Antagonistic effects of cofilin, beryllium fluoride complex, and phalloidin on subdomain 2 and nucleotide-binding cleft in F-actin. *Biophys. J.* 91:4490-4499.

Murakami, K., T. Yasunaga, T.Q.P. Noguchi, Y. Gomibuchi, K.X. Ngo, T.Q.P. Uyeda, and T. Wakabayashi. 2010. Structural basis for actin assembly, activation of ATP hydrolysis, and delayed phosphate release. *Cell.* 143:275-287.

Murthy, K., and P. Wadsworth. 2005. Myosin-II-dependent localization and dynamics of F-actin during cytokinesis. *Curr. Biol.* 15:724-731.

Nakashima, K., N. Sato, T. Nakagaki, H. Abe, S. Ono, and T. Obinata. 2005. Two mouse cofilin isoforms, muscle-type (MCF) and non-muscle type (NMCF), interact with F-actin with different efficiencies. *J. Biochem.* 138:519-526.

Nishida, E., S. Maekawa, and H. Sakai. 1984. Cofilin, a protein in porcine brain that binds to actin filaments and inhibits their interactions with myosin and tropomyosin. *Biochemistry*. 23:5307-5313.

Noguchi, T.Q.P., R. Toya, H. Ueno, K. Tokuraku, and T.Q.P. Uyeda. 2010a. Screening of novel dominant negative mutant actins using glycine targeted scanning identifies G146V actin that cooperatively inhibits cofilin binding. *Biochem Biophys Res Commun*. 396:1006-1011.

Noguchi, T.Q.P., Y. Gomibuchi, K. Murakami, H. Ueno, K. Hirose, T. Wakabayashi, and T.Q.P. Uyeda. 2010b. Dominant negative mutant actins identified in flightless Drosophila can be classified into three classes. *J. Biol. Chem.* 285:4337-4437.

Noguchi, T.Q.P., N. Kanzaki, H. Ueno, K. Hirose, and T.Q.P. Uyeda. 2007. A novel system for expressing toxic actin mutants in Dictyostelium and purification and characterization of a dominant lethal yeast actin

mutant. *J. Biol. Chem.* 282:27721-27727.

Oda, T., M. Iwasa, T. Aihara, Y. Maeda, and A. Narita. 2009. The nature of the globular- to fibrous-actin transition. *Nature*. 457:441-445.

Olson, T.M., V.V. Michels, S.N. Thibodeau, Y.S. Tai, and M.T. Keating. 1998. Actin mutations in dilated cardiomyopathy, a heritable form of heart failure. *Science*. 280:750-752.

Ono, S. 2007. Mechanism of depolymerization and severing of actin filaments and its significance in cytoskeletal dynamics. *Int Rev Cytol*. 258:1-82.

Ono, S. 2010. Dynamic regulation of sarcomeric actin filaments in striated muscle. *Cytoskeleton (Hoboken)*. 67:677-692.

Orlova, A., and E.H. Egelman. 1997. Cooperative rigor binding of myosin to actin is a function of F-actin structure. *J. Mol. Biol.* 265:469-474.

Pavlov, D., A. Muhlrad, J. Cooper, M. Wear, and E. Reisler. 2006. Severing of F-actin by yeast cofilin is pH-independent. *Cell Motil. Cytoskeleton*. 63:533-542.

Pollard, T.D. 2007. Regulation of actin filament assembly by Arp2/3 complex and formins. *Annu Rev Biophys Biomol Struct*. 36:451-477.

Pollard, T.D., L. Blanchoin, and R.D. Mullins. 2000. Molecular mechanisms controlling actin filament dynamics in nonmuscle cells. *Annu Rev Biophys Biomol Struct*. 29:545-576.

Riviere, J.B., B.W. van Bon, A. Hoischen, S.S. Kholmanskikh, B.J. O'Roak, C. Gilissen, S. Gijsen, C.T. Sullivan, S.L. Christian, O.A. Abdul-Rahman, J.F. Atkin, N. Chassaing, V. Drouin-Garraud, A.E. Fry, J.P. Fryns, K.W. Gripp, M. Kempers, T. Kleefstra, G.M. Mancini, M.J. Nowaczyk, C.M. van Ravenswaaij-Arts, T. Roscioli, M. Marble, J.A. Rosenfeld, V.M. Siu, B.B. de Vries, J. Shendure, A. Verloes, J.A. Veltman, H.G. Brunner, M.E. Ross, D.T. Pilz, and W.B. Dobyns. 2012. De novo mutations in the actin genes ACTB and ACTG1 cause Baraitser-Winter syndrome. *Nat Genet*. 44:440-444, S1-2.

Romet-Lemonne, G., and A. Jegou. 2013. Mechanotransduction down to individual actin filaments. *Eur J Cell Biol*. 92:333-338.

Schoenenberger, C.A., H.G. Mannherz, and B.M. Jockusch. 2011. Actin: from structural plasticity to functional diversity. *Eur J Cell Biol*. 90:797-804.

Sharma, S., E.E. Grintsevich, C. Hsueh, E. Reisler, and J.K. Gimzewski. 2012. Molecular cooperativity of drebrin1-300 binding and structural

remodeling of F-actin. *Biophys J.* 103:275-283.

Shu, X., N.C. Shaner, C.A. Yarbrough, R.Y. Tsien, and S.J. Remington. 2006. Novel chromophores and buried charges control color in mFruits. *Biochemistry*. 45:9639-9647.

Solomon, T.L., L.R. Solomon, L.S. Gay, and P.A. Rubenstein. 1988. Studies on the role of actin's aspartic acid 3 and aspartic acid 11 using oligodeoxynucleotide-directed site-specific mutagenesis. *J. Biol. Chem.* 263:19662-19669.

Spudich, J.A., and S. Watt. 1971. The regulation of rabbit skeletal muscle contraction. I. Biochemical studies of the interaction of the tropomyosin-troponin complex with actin and the proteolytic fragments of myosin. *J. Biol. Chem.* 246:4866-4871.

Sternlicht, H., G.W. Farr, M.L. Sternlicht, J.K. Driscoll, K. Willison, and M.B. Yaffe. 1993. The t-complex polypeptide 1 complex is a chaperonin for tubulin and actin in vivo. *Proc. Natl. Acad. Sci. U. S. A.* 90:9422-9426.

Straub, F.B. 1942. Actin. *Studies from the Institute of Medical Chemistry University Szeged*. 2:3-15.

Strohman, R.C. 1959. Studies on the enzymic interactions of the bound nucleotide of the bound nucleotide of the muscle protein actin. *Biochim Biophys Acta*. 32:436-449.

Strzelecka-Golaszewska, H. 1973. Effect of tightly bound divalent cation on the equilibria between G-actin-bound and free ATP. *Eur J Biochem*. 37:434-440.

Suarez, C., J. Roland, R. Boujemaa-Paterski, H. Kang, B.R. McCullough, A.C. Reymann, C. Guerin, J.L. Martiel, E.M. De la Cruz, and L. Blanchoin. 2011. Cofilin tunes the nucleotide state of actin filaments and severs at bare and decorated segment boundaries. *Curr Biol*. 21:862-868.

Theriot, J.A., and T.J. Mitchison. 1991. Actin microfilament dynamics in locomoting cells. *Nature*. 352:126-131.

Theriot, J.A., T.J. Mitchison, L.G. Tilney, and D.A. Portnoy. 1992. The rate of actin-based motility of intracellular Listeria monocytogenes equals the rate of actin polymerization. *Nature*. 357:257-260.

Tokuraku, K., R. Kurogi, R. Toya, and T.Q.P. Uyeda. 2009. Novel mode of cooperative binding between myosin and Mg2+ -actin filaments in the presence of low concentrations of ATP. *J Mol Biol*. 386:149-162.

Tsaturyan, A.K., N. Koubassova, M.A. Ferenczi, T. Narayanan, M. Roessle,

and S.Y. Bershitsky. 2005. Strong binding of myosin heads stretches and twists the actin helix. *Biophys. J.* 88:1902-1910.

Tsujioka, M., S. Yumura, K. Inouye, H. Patel, M. Ueda, and S. Yonemura. 2012. Talin couples the actomyosin cortex to the plasma membrane during rear retraction and cytokinesis. *Proc Natl Acad Sci U S A.* 109:12992-12997.

Uyeda, T.Q.P., Y. Iwadate, N. Umeki, A. Nagasaki, and S. Yumura. 2011. Stretching actin filaments within cells enhances their affinity for the myosin II motor domain. *PLoS One*. 6:e26200.

van den Ent, F., L. Amos, and J. Lowe. 2001. Bacterial ancestry of actin and tubulin. *Curr Opin Microbiol*. 4:634-638.

van Wijk, E., E. Krieger, M.H. Kemperman, E.M. De Leenheer, P.L. Huygen, C.W. Cremers, F.P. Cremers, and H. Kremer. 2003. A mutation in the gamma actin 1 (ACTG1) gene causes autosomal dominant hearing loss (DFNA20/26). *J. Med. Genet.* 40:879-884.

Volkmann, N., D. DeRosier, P. Matsudaira, and D. Hanein. 2001. An atomic model of actin filaments cross-linked by fimbrin and its implications for bundle assembly and function. *J Cell Biol*. 153:947-956.

Wegner, A. 1976. Head to tail polymerization of actin. *J Mol Biol*. 108:139-50.

Wegner, A. 1977. The mechanism of ATP hydrolysis by polymer actin. *Biophys Chem*. 7:51-58.

Wertman, K.F., D.G. Drubin, and D. Botstein. 1992. Systematic mutational analysis of the yeast ACT1 gene. *Genetics*. 132:337-350.

Williams, S.P., A.M. Fulton, and K.M. Brindle. 1993. Estimation of the intracellular free ADP concentration by 19F NMR studies of fluorine-labeled yeast phosphoglycerate kinase in vivo. *Biochemistry*. 32:4895-4902.

Woodrum, D.T., S.A. Rich, and T.D. Pollard. 1975. Evidence for biased bidirectional polymerization of actin filaments using heavy meromyosin prepared by an improved method. *J Cell Biol*. 67:231-237.

Yonezawa, N., E. Nishida, and H. Sakai. 1985. pH control of actin polymerization by cofilin. *J. Biol. Chem.* 260:14410-14412.

Yount, R.G., D. Babcock, W. Ballantyne, and D. Ojala. 1971. Adenylyl imidodiphosphate, an adenosine triphosphate analog containing a P--N--P linkage. *Biochemistry*. 10:2484-2489.

Yumura, S., H. Mori, and Y. Fukui. 1984. Localization of actin and myosin for

the study of ameboid movement in Dictyostelium using improved immunofluorescence. *J Cell Biol*. 99:894-899.

Zak, R., A.F. Martin, G. Prior, and M. Rabinowitz. 1977. Comparison of turnover of several myofibrillar proteins and critical evaluation of double isotope method. *J. Biol. Chem.* 252:3430-3435.

Zhu, M., T. Yang, S. Wei, A.T. DeWan, R.J. Morell, J.L. Elfenbein, R.A. Fisher, S.M. Leal, R.J. Smith, and K.H. Friderici. 2003. Mutations in the gamma-actin gene (ACTG1) are associated with dominant progressive deafness (DFNA20/26). *Am. J. Hum. Genet.* 73:1082-1091.